

**This is the preprint of the contribution published as:**

Zaryab, A., Nassery, H.R., **Knoeller, K.**, Alijani, F., Minet, E. (2022):  
Determining nitrate pollution sources in the Kabul Plain aquifer (Afghanistan) using stable isotopes and Bayesian stable isotope mixing model  
*Sci. Total Environ.* **823** , art. 153749

**The publisher's version is available at:**

<http://dx.doi.org/10.1016/j.scitotenv.2022.153749>

# **Determining nitrate pollution sources in the Kabul Plain aquifer (Afghanistan) using stable isotopes and Bayesian stable isotope mixing model**

Abdulhalim Zaryab<sup>ab</sup>, Hamid Reza Nassery<sup>a\*</sup>, Kay Knoeller<sup>c</sup>, Farshad Alijani<sup>a</sup>, Eddy Minet<sup>d</sup>

<sup>a</sup>Department of Minerals and Groundwater Resources, Faculty of Earth Sciences, Shahid Beheshti University, Evin Ave, Tehran, Iran

<sup>b</sup>Engineering Geology and Hydrogeology, Faculty of Geology and Mines, Kabul Polytechnic University, District 5, Kabul, Afghanistan

<sup>c</sup>Department Catchment Hydrology Helmholtz-Centre for Environmental Research – UFZ, D-06120 Halle, Germany

<sup>d</sup>Environmental Protection Agency (EPA), Dublin, Ireland

\*Corresponding author, E-mail address: h-nassery@sbu.ac.ir (H.R. Nassery), Phone: (+98)-90-2983-2399

1 **Determining nitrate pollution sources in the Kabul Plain aquifer (Afghanistan) using stable**  
2 **isotopes and Bayesian stable isotope mixing model**

3

4 Abdulhalim Zaryab<sup>ab</sup>, Hamid Reza Nassery<sup>a\*</sup>, Kay Knoeller<sup>c</sup>, Farshad Alijani<sup>a</sup>, Eddy Minet<sup>d</sup>

5 <sup>a</sup>Department of Minerals and Groundwater Resources, Faculty of Earth Sciences, Shahid Beheshti University, Evin  
6 Ave, Tehran, Iran

7 <sup>b</sup>Engineering Geology and Hydrogeology, Faculty of Geology and Mines, Kabul Polytechnic University, District 5,  
8 Kabul, Afghanistan

9 <sup>c</sup>Department Catchment Hydrology Helmholtz-Centre for Environmental Research – UFZ, D-06120 Halle, Germany

10 <sup>d</sup>Environmental Protection Agency (EPA), Dublin, Ireland

11 \*Corresponding author, E-mail address: h-nassery@sbu.ac.ir (H.R. Nassery), Phone: (+98)-90-2983-2399

12

13

14

15

16

17

18

19

20

21

22

23

24

26 **Abstract**

27 The Kabul urban aquifer (Afghanistan), which is the main source of drinking water for Kabul city's  
28 inhabitants, is highly vulnerable to anthropogenic pollution. In this study, the geochemistry of major ions  
29 (including reactive nitrogen species such as  $\text{NO}_3^-$ ,  $\text{NO}_2^-$ , and  $\text{NH}_4^+$ ) and stable isotope ratios ( $\delta^{15}\text{N}-\text{NO}_3^-$ ,  
30  $\delta^{18}\text{O}-\text{NO}_3^-$ ,  $\delta^{18}\text{O}-\text{H}_2\text{O}$ , and  $\delta^2\text{H}-\text{H}_2\text{O}$ ) of surface and groundwater samples from the Kabul Plain were  
31 analyzed over two sampling periods (dry and wet seasons). A Bayesian stable isotope mixing model  
32 (SIMMR) was also employed to trace potential nitrate sources, transformation processes and proportional  
33 contributions of nitrate sources in the Kabul aquifer. The plotting of  $\delta^{15}\text{N}-\text{NO}_3^-$  against  $\delta^{18}\text{O}-\text{NO}_3^-$  ( $\delta^{15}\text{N}-$   
34  $\text{NO}_3^-$  and  $\delta^{18}\text{O}-\text{NO}_3^-$  values ranged from +4.8 to +25.4‰ and from -11.7 to +18.6‰, respectively)  
35 suggests that  $\text{NO}_3^-$  primarily originated from the nitrification of sewage, and not from artificial fertilizer.  
36 High  $\text{Cl}^-$  concentrations and low  $\text{NO}_3^-/\text{Cl}^-$  ratios supported the assumption that sewage is the dominant  
37 nitrate source. The results indicated that denitrification did not influence the  $\text{NO}_3^-$  isotopic composition in  
38 the Kabul aquifer. The SIMMR model suggest that nitrate in the dry season originated mainly from  
39 sewage ~81%, followed by soil organic N 10.5%, and chemical fertilizer 8.5%. In the wet season, sewage  
40 ~87.5%, soil organic N 6.7%, and chemical fertilizer 5.8% were the main  $\text{NO}_3^-$  sources in the Kabul  
41 aquifer. Effective land management measures should be made to improve the sewage collection system in  
42 the Kabul Plain.

43 **Keywords:** Groundwater, Stable nitrate isotope, Nitrate, Bayesian stable isotope mixing model, Nitrogen  
44 transformation, Kabul

45

46 **1. Introduction**

47 The contamination of groundwater and surface water by nitrate ( $\text{NO}_3^-$ ) in urban and agricultural areas is a  
48 serious issue (Mayer et al., 2002; Voss et al., 2006; Kendall et al., 2007; Kaushal et al., 2011; Xu et al.,  
49 2015; Matiatos, 2016; Luu et al, 2020; Ye et al., 2021). From an environmental perspective, discharge of

50 contaminated groundwater into surface water bodies can contribute to eutrophic conditions in lakes,  
51 streams, estuaries and the coastal zone. From a health perspective, a high level of  $\text{NO}_3\text{-N}$  ( $> 10 \text{ mg L}^{-1}$ )  
52 in drinking water may result in blue baby syndrome in infants (methemoglobinemia) and also may  
53 contributing factor for some types of cancer (Fan and Steinberg, 1996; Gulis et al., 2002; Fewtrell, 2004;  
54 Ward et al., 2005; Pastén-Zapata et al., 2013; Nikolenko et al., 2017). While natural levels of nitrate in  
55 aquatic systems occurs at concentrations generally no higher than  $2.5 \text{ mg L}^{-1}$  as  $\text{NO}_3\text{-N}$  (Panno et al.,  
56 2006), higher  $\text{NO}_3$  concentrations are often the result of anthropogenic activities associated with  
57 excessive use of chemical fertilizers and manure by agriculture, sewage waste, and/or urban solid waste  
58 landfills (Kendall, 1998; Chang et al., 2002; Kendall et al., 2007; Xue et al., 2009; Pastén-Zapata et al.,  
59 2014; Kim et al., 2015; Popescu et al., 2015; Nikolenko et al., 2017; Mingming et al., 2018; Li et al.,  
60 2018; Soto et al., 2018; Ogrinc et al., 2018; Nejatijahromi et al., 2019; Zhang et al., 2020). Other factors  
61 may also affect nitrate concentrations such as temporal variability of rainfall, hydrogeological conditions  
62 and land cover (Exner-Kittridge et al., 2016; Suchy et al., 2018; Sebestyen et al., 2019; Romanelli et al.,  
63 2020).

64 Groundwater is a major source of freshwater worldwide and its use as drinking water in cities is  
65 increasing. Reducing  $\text{NO}_3$  pollution in groundwater is needed to improve, safe water usage, but to do so,  
66 it is important to accurately identify the origins of  $\text{NO}_3$  and quantify the contribution of nitrate sources.

67 Some  $\text{NO}_3$  sources exhibit characteristic  $^{15}\text{N}/^{14}\text{N}$  and  $^{18}\text{O}/^{16}\text{O}$  ratios (expressed as  $\delta^{15}\text{N-NO}_3$  and  $\delta^{18}\text{O-}$   
68  $\text{NO}_3$ ), which can provide valuable information to track the origin of nitrate contamination in aquatic  
69 environments (Böttcher et al., 1990; Wassenaar, 1995; Chang et al., 2002; Kendall et al., 2007; Xue et  
70 al., 2009; Nestler et al., 2011; Kim et al., 2015; Jung et al., 2020). Typically, chemical fertilizers and  
71 precipitation show the lowest  $\delta^{15}\text{N-NO}_3$  values, followed by soil-derived nitrate with intermediate values,  
72 and then nitrate derived from manure and sewage with the highest  $\delta^{15}\text{N-NO}_3$  values (Kendall et al., 2007,  
73 Xue et al., 2009). Over the last three decades, the addition of  $\delta^{18}\text{O-NO}_3$  has been successfully used by  
74 some to improve the identification of nitrate sources as well as nitrate attenuation processes in aquatic  
75 environments (Böttcher et al., 1990; Wassenaar, 1995; Aravena and Robertson, 1998; Kendall et al.,

76 2007; Savard et al., 2009; Liu et al., 2013; Ding et al., 2014; Griffiths et al., 2016; Yi et al., 2017; Li et  
77 al., 2018; Zendehbad et al., 2019; Zhao et al., 2019; Weitzman et al., 2021). However,  $\delta$  values can  
78 overlap between nitrate sources, which can complicate data interpretation. Furthermore, isotopic  
79 fractionation during the nitrate transformation processes, including nitrification and denitrification, can  
80 also alter the original isotopic compositions of nitrate sources (Kendall et al., 2007; Xue et al., 2009; Yi et  
81 al., 2017; Minet et al., 2017; Zhu et al., 2019; Zheng et al., 2020; Yang et al., 2020; Blarasin et al., 2020).  
82 Recently, the identification of nitrate sources was considerably improved by combining the dual stable  
83 isotope approach with hydrochemical and land use data (Pastén-Zapata et al., 2013; Minet et al., 2017;  
84 Biddau et al., 2018; Nejatijahromi et al., 2019, Wu et al., 2020).

85 Stable isotopes have also been used to quantify  $\text{NO}_3^-$  sources in aquatic systems. Early attempts involved  
86 a dual isotopic linear mixing model based on mass balance (Phillips and Koch, 2002; Deutsch et al.,  
87 2006). Nevertheless, this method presumed no significant isotopic fractionations from transformation  
88 processes and was limited to track no more than three sources (Parnell et al., 2010). Parnell et al. (2010)  
89 later implemented a Bayesian stable isotope mixing model in the software package SIAR (Stable Isotope  
90 Analysis in R). The Bayesian stable isotope mixing model was employed by Xue et al. (2012) to quantify  
91 nitrate sources for the first time. The SIAR model estimates the probability distribution of the  
92 proportional contributions based on the Bayesian approach and quantitatively identifies more than three  
93 nitrate sources, which overcomes earlier limitations of the linear isotopic mixing model (Parnell et al.,  
94 2010; Xue et al., 2012; Matiatos, 2016; Meghdadi and Javar, 2018; Li et al., 2019). During the past  
95 decade, other studies have combined stable isotopes in nitrate with a SIAR approach to identify the  
96 proportional contributions of  $\text{NO}_3^-$  sources in aquatic environments (Korth et al., 2014; Yang and Toor,  
97 2016; Jin et al., 2019; Torres-Martínez et al., 2020). However, limitations remain as the SIAR approach  
98 rarely considers the denitrification process and related fractionation (Xia et al., 2017; Meghdadi and  
99 Javar, 2017). To overcome these issues, Bayesian stable isotope mixing models (SIMMs) were developed  
100 (Parnell et al., 2013; Zhao et al., 2019) and used in a few recent studies that also combine hydrochemical

101 and land use data to more accurately identify and quantify the nitrate sources in aquatic systems (Zhang et  
102 al., 2020; Romanelli et al., 2020, Re et al., 2021; Torres-Martínez et al., 2021).

103 The study area, Kabul city, is located in southeast Afghanistan with a population of about 5.38 million  
104 inhabitants. Over the last two decades, it has experienced rapid unplanned urbanization. Groundwater is  
105 the only source of drinking water but its quality has long deteriorated due to (i) lack of centralized  
106 sewerage system, (ii) intensive fertilizer application and/or (iii) the direct discharge of solid waste in  
107 surface water. Some studies have been conducted before on groundwater quality of the Kabul Basin  
108 aquifer (Houben et al., 2005; Broshears et al., 2005; Mack et al., 2010; Saffi, 2019; Jawadi et al., 2020)  
109 and Houben et al., (2005) reported worryingly elevated nitrate concentrations ( $>350 \text{ mg L}^{-1}$ ). The  
110 determination of nitrate sources of nitrate and transformation processes were however less considered.  
111 This study aims to identify and quantify nitrate sources and associated biogeochemical processes using  
112 stable isotope ratios and a stable isotope mixing model (SIMMR) combined with land-use,  
113 hydrogeological and hydrochemical data.

114

## 115 **2. Material and Methods**

### 116 *2.1. Study area description*

117 The study area of Kabul city, the capital and the largest city in Afghanistan with an estimated population  
118 of approximately 5.38 million (NSIA, 2021) is located in the Kabul Plain in the center of the Kabul  
119 province in eastern Afghanistan. It covers an area of  $280 \text{ km}^2$  at an elevation of about 1800 m above sea  
120 level. (Fig. 1). The Plain is enclosed by low but quite steep mountain ranges, and it is divided into western  
121 and eastern plains by the Asmai and Share Darwaza mountains. Three major seasonal rivers flow through  
122 it: Kabul, Logar and Paghman (Fig.1). The western plain is drained from west to east by the upper Kabul  
123 and Paghman rivers and the eastern plain is drained by the Kabul and Logar rivers. The Kabul Plain is  
124 characterized by a semiarid climate with an average annual precipitation of 315 mm. The air temperature  
125 ranges from an average monthly low in January of  $-7^\circ\text{C}$  to an average monthly high in July of  $+32^\circ\text{C}$ . The  
126 rainy season, accounting for 68% of the annual rainfall, runs from January to April. The mountains

127 surrounding the Kabul Plain are mainly underlain by a variety of metamorphic rocks, which include,  
128 schist, gneiss and amphibolite, and sedimentary rocks, including limestone and dolomite (Bohannon,  
129 2010). The study area of Kabul city consists of an accumulation of terrestrial and lacustrine sediments,  
130 mainly of the Quaternary and Neogene ages.

131 The main land-uses in the Kabul Plain are residential (54.2% of the total area), followed by agriculture  
132 (20%), transportation (9.7%) and vacant plots (8.7%) (Fig. 2). The area under cultivation in the Kabul  
133 Plain covers about 56 km<sup>2</sup>. Agricultural land is mainly in the southwest of the Eastern Plain. The major  
134 crops of the Kabul Plain are wheat, potato, maize, millet, cucumber, vegetables and fruits. The chemical  
135 fertilizers used in the Kabul Plain ((Ministry of Agriculture, Irrigation and Livestock of Afghanistan,  
136 personal communication) are commonly imported by local suppliers from Pakistan, Iran, Turkey and  
137 China and their compositions are: urea (CO(NH<sub>2</sub>)<sub>2</sub>), ammonium sulfate (NH<sub>4</sub>)<sub>2</sub>SO<sub>4</sub>) and diammonium  
138 phosphate ((NH<sub>4</sub>)<sub>2</sub>HPO<sub>4</sub>). Besides chemical fertilizers, manures are also applied to crops. Chemical  
139 fertilizers are generally applied at the beginning (April) and in the middle of the growing season (June).  
140 Soil erosion is not a considerable process in the Kabul Plain (Safi et al., 2017). Based on land use  
141 information, potential sources of nitrate pollution in the plain are therefore anthropogenic and include  
142 sewage (pit latrines, septic tanks), intensive use of fertilizers (chemical fertilizers, manure and sewage  
143 sludge), solid waste landfill sites, solid waste disposal in the rivers and channels and presence of local  
144 cemeteries. It is important to note that there is currently no centralized sewerage system in Kabul city.  
145 Sewage collection and wastewater treatment plants operate only a small scale, particularly in areas like  
146 new townships (Paiman and Noori, 2019).

147 From a hydrogeological perspective, the Kabul Plain is thus divided into Quaternary and Neogene  
148 aquifers. The Quaternary aquifer, which was described in detail by Houben et al., (2009), is generally  
149 considered shallow and divided into three locally important interconnected Quaternary unconfined  
150 aquifers. It mainly consists of gravel and sandy beds covered by loess clay and silts beds with a thickness  
151 of up to a few meters. The thickness of this shallow aquifer can be up to 80 m. The hydraulic conductivity  
152 ranged from 4 to 112 m day<sup>-1</sup> (Houben et al., 2009). The Neogene aquifer, on the other hand, is deep and

153 semi-confined. It has a thickness that ranges between 30 and 600 m and is part of an aquitard/aquiclude  
154 (Houben et al., 2009; JICA, 2011; Landell Mills, 2020). The Neogene deep aquifer is composed of stiff  
155 clay with unconsolidated sand, gravel and conglomerates with a transmissivity ranging from 2 to 27 m<sup>2</sup>  
156 day<sup>-1</sup> (Landell Mills, 2020).

157 The major sources of groundwater recharge are infiltration of river channels, precipitation, and  
158 agricultural infiltration (water used for irrigation is supplied by rivers and groundwater), while  
159 groundwater discharge is largely accounted for by pumping withdrawals for drinking, agricultural and  
160 industrial uses. Due to over-abstraction, groundwater now flows toward the central part of the western  
161 plain, whereas it used to be directed from west and south-east toward the east (Brohears et al., 2005). The  
162 groundwater flow direction in the eastern plain is from south and west toward the east and from the  
163 central part of the plain to the northwest. It can be noted that with the recent and rapid urbanization of  
164 Kabul city, groundwater abstraction has increased dramatically and the groundwater table depth in the  
165 Plain has declined rapidly (-1.7 m/year on average) (Zaryab et al., 2017).

166

## 167 *2.2. Sampling and analyses*

168 After consideration of the different land uses, potential sources of pollution, and hydrogeological  
169 conditions, twenty-nine wells were selected for groundwater sampling, (Fig. 2). These water wells range  
170 in depth between 20 to 120 m (Table S1). Water samples were collected during two sampling campaigns  
171 conducted in the dry (November 2020) and in the wet seasons (April 2021). Before collecting the  
172 samples, each well was purged for up to 10 min, until all field parameters had stabilized. Other water  
173 samples that were collected included river water (Paghman, Kabul, and Logar Rivers), mixed wastewater  
174 and irrigation return flows. Field measurements, recorded with a pre-calibrated hand-held meter (Multi  
175 340i, WTW, Germany), included pH, dissolved oxygen (DO), temperature and electrical conductivity  
176 (EC). Each water sample was split into three aliquots that were analyzed for either nitrogenous nutrients  
177 (NO<sub>3</sub><sup>-</sup>, NO<sub>2</sub><sup>-</sup>, NH<sub>4</sub><sup>+</sup>), major ions (Ca<sup>2+</sup>, Mg<sup>2+</sup>, Na<sup>+</sup>, K<sup>+</sup>, HCO<sub>3</sub><sup>-</sup>, Cl<sup>-</sup>, SO<sub>4</sub><sup>2-</sup>) or stable isotope signatures in  
178 nitrate ( $\delta^{15}\text{N-NO}_3^-$ ,  $\delta^{18}\text{O-NO}_3^-$ ). In addition, thirty-two groundwater and surface-water samples collected

179 during the wet season were analyzed for stable isotope signatures in water only ( $\delta^2\text{H-H}_2\text{O}$  and  $\delta^1\text{H-H}_2\text{O}$ )  
180 and  $^{18}\text{O}/^{16}\text{O}$  ratios in  $\text{H}_2\text{O}$ ). Nutrient concentrations were measured with a spectrophotometer (DR 5000,  
181 Hach, USA) on samples collection day at the Green Tech Laboratory in Kabul. Aliquots for major ions  
182 analysis were shipped to the Regional Water Organization Laboratory of Tehran (Iran). The measurement  
183 of parameters other than bicarbonate ( $\text{HCO}_3^-$ ) was carried out by ion chromatography (S 151 IC, Sykam,  
184 Germany), as per APHA (2017).  $\text{HCO}_3^-$  concentrations were determined using the titration method  
185 outlined by Stumm and Morgan (2012). Some duplicates and field blanks were also collected and  
186 analyzed for quality assurance purposes. The reliability of all the chemical analyses was checked by ionic  
187 charge balance, with a threshold error of 5 % set to accept results. All the gathered data, including in situ  
188 measurements, ion concentrations, and isotopes ratios are presented in Table S1. The statistical summary  
189 of the data is listed in Table 2.

190 Aliquots for stable isotopes analysis in nitrate were filtered on-site into 60 mL HDPE bottles with 0.22  
191  $\mu\text{m}$  cellulose filters, which aimed at removing particulate matter and most microbial activity that could  
192 cause some isotopic fractionation. Samples were kept refrigerated until they were shipped to the  
193 Helmholtz Centre for Environmental Research-UFZ (Germany). Dual stable isotope analysis (i.e.  $^{15}\text{N}/^{14}\text{N}$   
194 and  $^{18}\text{O}/^{16}\text{O}$  ratios in  $\text{NO}_3^-$ , referred to as  $\delta^{15}\text{N-NO}_3$  and  $\delta^{18}\text{O-NO}_3$ , respectively) were carried out in  
195 duplicate for each sample on a GasbenchII/delta V plus combination (Thermo Scientific, USA) using the  
196 denitrifier method for a simultaneous determination of  $\delta^{15}\text{N}$  and  $\delta^{18}\text{O}$  in the measuring gas  $\text{N}_2\text{O}$ , produced  
197 by controlled reduction of sample nitrate (Sigman et al., 2001; Casciotti et al., 2002). Nitrogen and  
198 oxygen stable isotope results are reported in delta ( $\delta$ ) notation ( $\delta_{\text{sample}} = [(R_{\text{sample}}/R_{\text{standard}}) - 1] \times 1000$ ) as  
199 part per thousand (‰) deviation relative to the standards AIR for nitrogen and Vienna Standard Mean  
200 Ocean Water (VSMOW) for oxygen, where R is the ratio of the heavy to light isotope (i.e.  $^{15}\text{N}/^{14}\text{N}$  and  
201  $^{18}\text{O}/^{16}\text{O}$ ). The standard deviation of the described analytical measurement was  $\pm 0.4$  ‰ for  $\delta^{15}\text{N}$  and  $\pm 1.6$   
202 ‰ for  $\delta^{18}\text{O}$ . Stable isotope results in Section 3 represent the mean value of duplicated measurements for  
203 each sample.

204 Aliquots for stable isotopes analysis in water were also filtered on-site into 60 HDPE bottles with 0.22  $\mu\text{m}$   
205 cellulose filters and shipped to the Helmholtz Centre for Environmental Research-UFZ. Dual stable  
206 isotope analyses ( $^2\text{H}/^1\text{H}$  and  $^{18}\text{O}/^{16}\text{O}$  ratios in  $\text{H}_2\text{O}$ , referred to as  $\delta^2\text{H}\text{-H}_2\text{O}$  and  $\delta^{18}\text{O}\text{-H}_2\text{O}$ , respectively)  
207 were carried out using laser cavity ring-down spectroscopy (Picarro L2120-I, Santa Clara, USA) without  
208 further treatment of the water samples. Results were reported in  $\delta$  values relative to VSMOW. Samples  
209 were normalized to the VSMOW scale using replicate (20x) analysis of internal standards calibrated to  
210 VSMOW and Standard Light Antarctic Precipitation (SLAP) certified reference materials. The analytical  
211 uncertainty of the  $\delta^{18}\text{O}$  measurement was  $\pm 0.1\text{‰}$ , for hydrogen isotope analyses, an analytical error of  
212  $\pm 0.8\text{‰}$  has to be considered.

213 ArcGIS tools were employed to represent the spatial variations of nitrate concentrations and values of  
214  $\delta^{15}\text{N}\text{-NO}_3^-$ ,  $\delta^{18}\text{O}\text{-NO}_3^-$ . AqQA software was used to characterize of hydrochemical facies of the water  
215 samples. All the scatter diagrams were created using Microsoft Excel 2019.

216

### 217 *2.3. Estimation of contributions from different nitrate pollution sources*

218 The proportional contributions of the different  $\text{NO}_3$  sources in the water samples were calculated using a  
219 Bayesian Stable Isotope Mixing Model (SIMMR) package for R, and an updated version of the Bayesian  
220 isotope mixing model named SIAR. The methodology employed in the SIMMR model has been  
221 described in detail by Parnell et al. (2013) and Parnell (2016). This approach can incorporate sources of  
222 uncertainty, isotope fractionation, and multiple  $\text{NO}_3$  sources (Parnell et al., 2013; Zhao et al., 2019;  
223 Herms et al., 2021). The SIAR model is an open-source software package for R and uses the Markov  
224 chain Monte Carlo method to estimate possible source proportions. By defining, a set of N mixture  
225 measurements on j stable isotopes with k source contributors are expressed as follows:

$$226 \quad X_{ij} = \sum_{k=1}^K P_k(S_{jk} + C_{jk}) + \varepsilon_{ij}$$

$$227 \quad S_{jk} \sim N(\mu_{jk}, \omega_{jk}^2)$$

$$228 \quad C_{jk} \sim N(\lambda_{jk}, \tau_{jk}^2)$$

$$229 \quad \varepsilon_{jk} \sim N(0, \sigma_j^2)$$

230 where  $X_{ij}$  is the isotope value  $j$  of the mixture  $i$ , in which  $i = 1, 2, 3, \dots, N$  and  $j = 1, 2, 3, \dots, J$ ;  $S_{jk}$  is the  
231 source value  $k$  based on isotope  $j$  ( $k = 1, 2, 3, \dots, K$ ) and is normally distributed with the mean  $\mu_{jk}$  and the  
232 standard deviation  $\omega_{jk}$ ;  $P_k$  is the proportion of source  $k$ , as estimated by the SIAR model;  $C_{jk}$  is the  
233 fractionation factor for isotope  $j$  on source  $k$  and is normally distributed with mean  $\lambda_{jk}$  and standard  
234 deviation  $\tau_{jk}$ ; and  $\varepsilon_{ij}$  is the residual error, representing the additional unquantified variation between  
235 individual mixtures and is normally distributed with a mean of 0 and a standard deviation  $\sigma_j$ .

236 The SIMMR model was conducted in the SIMMR package of the R Programming Language (version 4.1)  
237 in the RStudio environment. The different isotopic signatures of nitrate sources employed in the SIMMR  
238 were obtained through a literature review and local end-members (Xue et al., 2009; Nikolenko et al.,  
239 2018; Zhang et al., 2018; Torres-Martínez et al., 2020). These values are listed in Table 1.

240

### 241 **3. Results and discussion**

#### 242 *3.1. Hydrochemistry*

243 The in-situ measurements, chemical parameters, and isotopic ratios measured in the groundwater and  
244 river water samples collected from the Kabul Plain are presented in Table S1 of the supplementary  
245 material. pH in both seasons was very similar and slightly alkaline. It ranged from 7.0 to 8.1 (mean value  
246 of 7.6) in the dry season (November 2020), and from 7.1 to 8.0 (mean of 7.6) in the wet season (April  
247 2021). EC ranged from 618 to 17830  $\mu\text{S cm}^{-1}$  (mean of 1640  $\mu\text{S cm}^{-1}$ ) in the dry season, and from 458 to  
248 16430  $\mu\text{S cm}^{-1}$  in the wet season (mean of 1430  $\mu\text{S cm}^{-1}$ ). The elevated EC values were encountered in  
249 the lacustrine evaporite deposits (Zaryab et al., 2021). The temperature of water samples ranged from 6°C  
250 to 17.8°C (mean value of 15.4°C) in the dry season and from 12.7°C to 18°C (mean value: 16.2°C) in the  
251 wet season. Dissolved oxygen (DO) concentration varied from 2.1 to 9.6  $\text{mg L}^{-1}$  (mean 5.3  $\text{mg L}^{-1}$ ) in the  
252 dry season, and from 1.9 to 8.3  $\text{mg L}^{-1}$  (mean 4.8  $\text{mg L}^{-1}$ ) in the wet season, indicating aerobic conditions  
253 in the aquifer. The elevated DO contents in the dry and wet seasons, could possibly be due to the presence  
254 of thousands of water wells in the Kabul Plain with long screens and excessive pumping from these wells.

255 In most groundwater samples of the western plain, the dominant cations were  $\text{Ca}^{2+} > \text{Mg}^{2+} > \text{Na}^+ > \text{K}^+$ ,  
256 whereas the dominant anions were  $\text{HCO}_3^- > \text{Cl}^- > \text{SO}_4^{2-}$ . In comparison,  $\text{Mg}^{2+}$  was the dominant cation in  
257 most groundwater samples of the eastern aquifer. High concentrations of  $\text{Mg}^{2+}$  might be due to the  
258 dissolution of dolomite (Zaryab et al., 2021). Major ion concentrations of groundwater samples were  
259 plotted in a Piper diagram (Fig. 3) to characterize hydrochemical dominant groundwater types in the  
260 Kabul aquifer. As shown in Fig. 3a and 3b, groundwater collected in both November 2020 and April 2021  
261 displays similar patterns. Based on the Piper diagram, the dominant type of groundwater in the western  
262 plain is  $\text{Ca-HCO}_3$ , followed by  $\text{Ca-(Mg, Na)-HCO}_3$ . In the eastern plain, the dominant type of water is  
263  $\text{Mg-HCO}_3$ , followed by  $\text{Mg-(Na, Ca)-HCO}_3(\text{Cl, SO}_4)$ ,  $\text{Na-SO}_4$ , and  $\text{Na-Cl}$  water types. Except for  
264 sampling well W5, all groundwater samples in the western plain displayed freshwater facies. On the other  
265 hand, most of the groundwater samples in the eastern plain demonstrate brackish water facies.

266

### 267 3.2. Isotopic compositions of water

268 The isotopic composition was used to assess the interactions between groundwater and rivers to identify  
269 the origins of water in the study area (Cook, 2013; Clark, 2015). Values of  $\delta^2\text{H-H}_2\text{O}$  and  $\delta^{18}\text{O-H}_2\text{O}$  in  
270 groundwater and river water samples from the Kabul Plain are presented in Table S1 of the  
271 supplementary material. The values of  $\delta^2\text{H-H}_2\text{O}$  and  $\delta^{18}\text{O-H}_2\text{O}$  in groundwater ranged from -73.4‰ to -  
272 30.3‰ (mean of -52.2‰) and -10.59‰ to -6.39‰ (mean of -8.31‰), respectively. The values of  $\delta^2\text{H-}$   
273  $\text{H}_2\text{O}$  and  $\delta^{18}\text{O-H}_2\text{O}$  in the rivers varied from -53.9‰ to -43.3‰ and -8.50‰ to -7.37‰, respectively. As  
274 shown in Fig. 4, most of the water samples fall above the global meteoric water line ( $\delta^2\text{H} = 8.13\delta^{18}\text{O} +$   
275  $10.8$ ) (Rozanski et al., 1993) and to below the local meteoric water line ( $\delta^2\text{H} = 7.325\delta^{18}\text{O} + 12.37$ ), which  
276 is based on IAEA data (1962-1989) reported by Houben et al. (2005). Generally, the deviation of the local  
277 meteoric water line from the global meteoric water line is controlled by an element-specific fractionation  
278 of the stable water isotopes along the vapor mass trajectory due to (1) latitudinal effect (lower delta values  
279 at increasing latitude), (2) continental effect (lower delta values the more inland), (3) altitude effect  
280 (lower delta values at higher altitude, (4) seasonal effect (lower delta values in winter in temperate

281 regions) and (5) amount effect (lower delta values during heavy storms (Mook and de Vries, 2000). The  
282 deviation of the water isotopic values of the groundwater from the local meteoric water line may be due to  
283 the occurrence of evaporation. This means that groundwater is isotopically enriched with respect to local  
284 precipitation due to evaporation. Therefore, the local rainfall after evaporation is the major source of  
285 groundwater in the Kabul Plain. Fig. 4 shows that except for water samples W4, W15 and W24 all  
286 groundwater samples followed the same pattern. The water well W4 experienced a rapid water table  
287 decline in recent years due to low permeability of subsurface soil (Meldebekova et al., 2020). It reveals  
288 that low  $\delta^{18}\text{O}$  and  $\delta^2\text{H}$  values in water well W4 reflect long groundwater residence times and recharge  
289 during colder climates in the past. It should be mentioned that the water table in the northwest of the study  
290 area also dramatically declined in recent years due to the low permeability of the aquifer (Landell Mills,  
291 2020), but the groundwater flow direction (Fig. 1) indicates that groundwater mixing occurred in the  
292 mentioned area. Water wells W15 and W24 are drilled within the lacustrine evaporite deposits. Therefore,  
293 isotopically-depleted groundwater sample W15 and enrichment in  $\delta^{18}\text{O}$  and  $\delta^2\text{H}$  of groundwater sample  
294 W24 might be because of high salinity in groundwater and exchange with rock minerals, respectively  
295 (Clark, 2015; Domenico and Schwartz, 1990). The isotopic compositions of groundwater clearly reflected  
296 the rate of recharge from rivers and rainfall and the effects of evaporation in the Kabul aquifer. In general,  
297 the  $\delta^2\text{H-H}_2\text{O}$  and  $\delta^{18}\text{O-H}_2\text{O}$  values indicated that most groundwater in the Kabul aquifer was recharged  
298 under similar climatic conditions.

299 The river water sample from Paghman River (PR) plots on the local meteoric water line (LMWL), while  
300 two other river water samples (Kabul River (KR) and Logar River (LR)) plot in a more isotopically  
301 enriched range similar to the groundwater samples. It suggests that Kabul and Logar rivers evaporated  
302 along their flow directions, because before entering the Kabul Plain, they flow long distances compared to  
303 the Paghman River. In the meantime, Fig. 4 indicates that the Kabul River originates from a higher  
304 altitude because this river was more depleted in  $\delta^{18}\text{O}$  and  $\delta^2\text{H}$  than Paghman and Logar rivers. The  
305 isotopic compositions of rivers indicate that the rivers also are the main source of groundwater in the  
306 Kabul Plain.

307

308 *3.3. Concentrations and isotopic compositions of nitrate*

309 The concentrations and isotopic compositions of nitrate in water samples of the Kabul Plain are listed in  
310 Table S1 (no isotopic values for well W20). The  $\delta^{15}\text{N-NO}_3$  values in groundwater samples from 28  
311 different locations in the Kabul aquifer ranged from 4.8‰ to 20.8‰ (mean of 10.2‰) in the dry season  
312 (November 2020) and from 6.9‰ to 25.4‰ (mean of 12.8‰) in the wet season (April 2021). The  $\delta^{18}\text{O-}$   
313  $\text{NO}_3$  values varied from -11.7‰ to 18.6‰ (mean of 7.2‰) in the dry season and from -3.4‰ to 11.5‰  
314 (mean of 4‰) in the wet season. The  $\delta^{15}\text{N-NO}_3$  in rivers' water varied between 7.7‰ and 10.2‰, whereas  
315  $\delta^{18}\text{O-NO}_3$  varied between -3.4‰ and 5.3‰. The  $\delta^{18}\text{O-NO}_3$  spanned a wide range (-11.7 to 18.6‰) in the  
316 dry season and relatively narrowed (-3.4 to 11.5‰) in the wet season (Table S1). The observed wide  
317 range of  $\delta^{18}\text{O-NO}_3$  values in the dry season might be due to the application of chemical fertilizers in  
318 agricultural lands and the mixing of water with different  $\text{NO}_3$  loads. The  $\delta^{15}\text{N-NO}_3$  and  $\delta^{18}\text{O-NO}_3$  values  
319 of mixed wastewaters and mixed irrigation water ranged from 14.4‰ to 13.6‰ and 11‰ to -4.1‰,  
320 respectively. The high  $\delta^{15}\text{N-NO}_3$  value in the mixed irrigation water sample could be due to using sewage  
321 sludge as fertilizer in agricultural areas. The  $\text{NO}_3$  concentrations spanned a wide range of values, from 4  
322 to 120.4 mg L<sup>-1</sup> in the dry season (mean value 13.7 mg L<sup>-1</sup>) and from 4.9 to 59 mg L<sup>-1</sup> in the wet season  
323 (mean of 17.71 mg L<sup>-1</sup>). All nitrate concentrations were above (and often widely above) the threshold  
324 value for anthropogenic activity (2.5 mg L<sup>-1</sup>) (Panno et al., 2006; Ogrinc et al., 2019), which can most  
325 likely be linked to human activities in the study area (Broshears et al., 2005; Houben et al., 2008). The  
326 high  $\delta^{15}\text{N-NO}_3$  values suggest that urban sewage was a major source of nitrate in the area (Kendall, 1998;  
327 Mayer et al., 2002; Xue et al., 2009, Xu et al., 2016). It is worth mentioning that nitrate concentrations in  
328 the groundwater of the Kabul aquifer decreased in comparison to the results reported in previous studies  
329 (Broshears et al., 2005; Houben, et al., 2005). It might be due to a significant decline in groundwater  
330 tables in densely populated areas (Khair Khana and Dashti Barchi). The nitrite concentrations ranged  
331 from 0.01 to 2.8 mg L<sup>-1</sup> and from 0.01 to 0.36 mg L<sup>-1</sup> with average values of 0.22 and 0.03 mg L<sup>-1</sup> in the  
332 dry and with the season, respectively (Table S1).

333

334 *3.4. Spatial variations of nitrate concentrations and isotope values*

335 The spatial variations in the concentration of  $\text{NO}_3$ ,  $\delta^{15}\text{N-NO}_3$  and  $\delta^{18}\text{O-NO}_3$  values in groundwater of the  
336 Kabul aquifer for both dry and wet seasons are illustrated in Fig. 5. The highest observed concentration of  
337 nitrate in the dry season was  $120.4 \text{ mg L}^{-1}$  in well W12, while the lowest observed concentration of  
338 nitrate was  $4 \text{ mg L}^{-1}$  in well W20. The highest and lowest concentrations of nitrate ( $58.9$  and  $4.87 \text{ mg L}^{-1}$ )  
339 were detected at wells W27 and W7, respectively. The field survey reveals that sewage waste may have  
340 caused high concentrations of nitrate in groundwater wells W12 and W27. Elevated nitrate ( $50.9 \text{ mg L}^{-1}$ )  
341 in well W1 in the dry season might be associated with agricultural activities and the presence of a local  
342 cemetery. The  $\text{NO}_3$  concentrations were generally higher during the wet season compared to the dry  
343 season in the study area. However,  $\text{NO}_3$  concentration in well W12 considerably decreased in the wet  
344 season compared to its concentration in the dry season. In general, the spatial distribution of nitrate  
345 concentrations in the Kabul aquifer in the dry and wet seasons does not reveal any clear picture. About  
346 70% of the groundwater samples showed nitrate concentrations exceeding  $2.5 \text{ mg L}^{-1}$  as  $\text{NO}_3\text{-N}$ , the  
347 threshold considered as a result of anthropogenic activity (Panno et al., 2006), and about 6% of the  
348 groundwater samples showed nitrate concentrations above the threshold value ( $50 \text{ mg L}^{-1}$ ) as set by the  
349 WHO (WHO, 2017). This highlights the significant influence of anthropogenic  $\text{NO}_3$  inputs on  
350 groundwater quality in the Kabul aquifer. Decreasing nitrate concentration and increasing  $\delta^{15}\text{N-NO}_3$  value  
351 in the northern part of the study area in the wet season may be associated with volatilization of  $^{15}\text{N}$ -  
352 depleted ammonia and mixing processes (Kendall et al., 2007; Biddau et al., 2019). The low  $\text{NO}_3$   
353 concentration in sample W12 could be also due to low  $\text{NH}_4^+$  concentrations (Fadhullah et al., 2019). The  
354 high  $\delta^{15}\text{N-NO}_3$  values ( $>10\text{‰}$  in average) were detected in most collected groundwater samples in both  
355 dry and wet seasons, suggesting that sewage and to a lesser extent manure inputs were probably  
356 responsible for the high nitrogen isotope ratios of nitrate in the urban aquifer of the Kabul city. Overall,  
357 higher  $\delta^{15}\text{N-NO}_3$  values were typically detected in the wet season. It could be explained by volatilization  
358 processes that may affect sewage and  $\text{NH}_4^+$  fertilizer and mixing processes (Shalev et al., 2015; Biddau et

359 al., 2019; Torres-Martínez et al., 2021). Generally, higher  $\delta^{18}\text{O}-\text{NO}_3$  values were observed in the dry  
360 season compared with the wet season. This pattern may be associated with evaporation in the dry season  
361 (Kendall et al., 2007; Shalev et al., 2015). From this, it can be concluded that the isotopic composition of  
362 nitrate in the study area is to an extent impacted by the hydrological regime.

363

### 364 *3.5. Using dual isotopes to identify nitrate sources*

365 In this study,  $\delta^{15}\text{N}-\text{NO}_3$  and  $\delta^{18}\text{O}-\text{NO}_3$  values (Fig. 6) were employed to identify the dominant potential  
366 sources of nitrate in the Kabul aquifer (Kendall et al., 2007). Almost all groundwater samples plotted in  
367 manure/sewage waste area, which suggests that sewage and septic wastes, and to lesser extent manure are  
368 the main contributors of nitrate in the plain with significant urban land use (Fig. 6). Almost all  
369 groundwater samples have  $\delta^{15}\text{N}-\text{NO}_3$  values above +7‰ in the dry and wet seasons, which suggests that  
370 most of the nitrate in the Kabul aquifer is derived from sewage sources (Fig. 6). Chemical fertilizers did  
371 not appear to be a considerable contributor, although  $\delta^{15}\text{N}-\text{NO}_3$  values below +7‰ indicate a mixture of  
372 sewage waste and soil N in wells W3 and W4, and sewage and ammonium fertilizer in well W21. It is  
373 worth mentioning that a mixture of nitrate from different sources is in good agreement with land-use data  
374 (Fig. 2), where different N source types coexist. Therefore,  $\text{NO}_3$  in the Kabul Plain should primarily be  
375 influenced by the mixing of at least three sources (Sewage, soil organic N and chemical fertilizers). The  
376  $\text{NO}_3/\text{Cl}$  molar ratios and  $\delta^{15}\text{N}-\text{NO}_3$  data also were used to identify the major sources of nitrate in the  
377 Kabul Plain (Yue et al., 2014). According to Fig.7b, most of the water samples in both seasons displayed  
378 relatively high  $\text{NO}_3/\text{Cl}$  molar ratios with  $\delta^{15}\text{N}-\text{NO}_3$  values greater than 8‰, suggesting that  $\text{NO}_3$  was  
379 originated mainly from nitrification sewage and septic wastes.

380

### 381 *3.6. Biogeochemical processes controlling nitrate fate*

382 Besides the influence of various nitrate sources that have characteristics of isotopic compositions, the  
383 isotopic composition of groundwater nitrate is also affected by biogeochemical processes. A theoretical  
384  $\delta^{18}\text{O}-\text{NO}_3$  value produced by microbial nitrification in an aerobic environment was determined using the

385  $\delta^{18}\text{O-H}_2\text{O}$  values measured for the surface and groundwater in the Kabul Plain (Table S1 in the  
386 supplementary material), assuming  $\delta^{18}\text{O}$  of atmospheric  $\text{O}_2$  (23.5‰) based on the following equation  
387 (Anderson and Hooper, 1983, Kendall et al., 2007).

388  
389 
$$\delta^{18}\text{O-NO}_3 = 2/3(\delta^{18}\text{O-H}_2\text{O}) + 1/3(\delta^{18}\text{O-air})$$

390  
391 For simplification of the equation, we did not consider any potential oxygen isotope exchange of  
392 intermediates with the ambient water during nitrification as proposed by Casciotti and Buchwald (2012).  
393 As shown in Fig. 7a, the calculated oxygen isotopic compositions for most samples in the wet season plot  
394 are close to the theoretical nitrification trend, which suggests that nitrification is the main process forming  
395 dissolved nitrate in the Kabul Plain. The DO concentrations also confirm that the nitrification process  
396 could be the major source of nitrate in the Kabul Plain (Table S1). For the other groundwater samples, the  
397  $\delta^{18}\text{O-NO}_3$  values plot far from the theoretical nitrification line, suggesting that other processes are also  
398 involved (Fig. 7a). Some samples (LR, W25, W9, and W6) showed slightly lower  $\delta^{18}\text{O-NO}_3$  values than  
399 the theoretical nitrification line. This observation might be explained by oxygen isotope exchange  
400 between intermediates during nitrification and ambient  $\text{H}_2\text{O}$ , which could alter the oxygen isotopic  
401 composition of nitrate in soil and lead to low values of  $\delta^{18}\text{O-NO}_3$  in water (Kool et al., 2011; Wexler et  
402 al., 2012). A few samples tended to exhibit slightly higher  $\delta^{18}\text{O-NO}_3$  values than to the theoretical  
403 nitrification line, which could be attributed to the incorporation of oxygen from water with high  $\delta^{18}\text{O-H}_2\text{O}$   
404 values (because of evaporation of soil waters or bacterial respiration) (Yue et al., 2014; Biddau et al.,  
405 2019; Torres-Martínez et al., 2021). Moreover, Fig. 7a shows that  $\delta^{18}\text{O-NO}_3$  values for water samples of  
406 the Kabul Plain are far below the atmospheric oxygen line characteristic for atmospheric nitrate,  
407 suggesting that nitrification is the main process forming dissolved nitrate in the Kabul aquifer (Meghdadi  
408 and Javar, 2018, Yang et al., 2020; Torres-Martínez et al., 2021).

409 The  $\delta^{15}\text{N-NO}_3$  values used in combination with of  $\text{NO}_3/\text{Cl}$  molar ratios were also employed to investigate  
410 microbial processes in the Kabul Plain. As shown in Fig. 7b, most samples from the dry and wet seasons  
411 plot in a range characteristic of nitrification, indicating that nitrification is the main process forming

412 dissolved nitrate in the Kabul aquifer (Table S1). Two samples (KR and W21) revealed medium  $\text{NO}_3/\text{Cl}$   
413 molar ratios with  $\delta^{15}\text{N-NO}_3$  values lower than 5.5‰, suggesting that  $\text{NO}_3$  may be derived from  
414 ammonium fertilizer in the dry season, which was also confirmed by land-use information (Fig. 2). A few  
415 samples in both dry and wet seasons displayed medium to high  $\text{NO}_3/\text{Cl}$  molar ratios with  $\delta^{15}\text{N-NO}_3$   
416 values between 5‰ and 8‰, suggesting that  $\text{NO}_3$  was primarily derived from soil organic N (Fig. 7b)  
417 (Torres-Martínez et al., 2021). Most of the samples in both dry and wet seasons exhibited relatively high  
418  $\text{NO}_3/\text{Cl}$  molar ratios with  $\delta^{15}\text{N-NO}_3$  values greater than 8‰, indicating that  $\text{NO}_3$  was affected directly by  
419 sewage and septic wastes (Fig. 7b). Moreover, some samples in the central and north-west of the eastern  
420 plain showed relatively low  $\text{NO}_3/\text{Cl}$  molar ratios with  $\delta^{15}\text{N-NO}_3$  values greater than 15‰ (Fig. 7b),  
421 suggesting that  $\text{NO}_3$  may originate from sewage waste and also that ammonia volatilization and mixing  
422 processes might have occurred in the mentioned areas (Kendall et al., 2007; Widory et al., 2013; Biddau  
423 et al., 2019; Torres-Martínez et al., 2021).

424 Further analysis of the potential sources of nitrate in the Kabul aquifer depends on the presence/absence  
425 of denitrification. Denitrification causes a significant reduction of  $\text{NO}_3$  concentrations and increases  $\delta^{15}\text{N-}$   
426  $\text{NO}_3$  and  $\delta^{18}\text{O-NO}_3$  values of the residual  $\text{NO}_3$  (Böttcher et al., 1990; Rivett et al., 2008; Hocaoglu et al.,  
427 2011). Regression analyses reveal that  $\delta^{15}\text{N-NO}_3$  had a weak positive relationship with  $\delta^{18}\text{O-NO}_3$  in the  
428 dry season ( $R^2 = 0.16$ ,  $p < 0.05$ , slope = 0.65,  $n = 28$ ) and in the wet season ( $R^2 = 0.22$ ,  $p < 0.05$ , slope =  
429 0.46,  $n = 31$ ) (Fig. 6). The slope of the linear regression line for the dry season was within the reported  
430 ranges of denitrification (0.5 – 1) (Mayer et al., 2002; Kendall et al., 2007), however, the water samples  
431 were not plotted along the 2:1 or 1:1 denitrification line. Therefore, the volatilization and mixing  
432 processes might be responsible for the slight isotopic enrichment of  $\delta^{15}\text{N-NO}_3$  and  $\delta^{18}\text{O-NO}_3$  during the  
433 dry season (Biddau et al., 2019, Yue et al., 2014). Overall, denitrification processes did not have a  
434 significant impact on the nitrate isotopic composition in the Kabul Plain in the dry and wet seasons (Ding  
435 et al., 2014). DO concentrations (Table S1) also confirm the limitation of denitrification processes in the  
436 Kabul aquifer (Orginc et al., 2019). However, a recent study by Utom et al. (2020) indicated that the

437 denitrification process does not always happen under strictly anoxic conditions, as it is commonly  
438 assumed.

439 Moreover, the relationships of  $\delta^{15}\text{N-NO}_3$  and  $\delta^{18}\text{O-NO}_3$  versus  $1/[\text{NO}_3^-]$  were employed to further assess  
440 the mixing and denitrification processes that may have occurred in the Kabul aquifer. The Keeling plots  
441 (Fig. 8a-b) displayed concentrations of  $\text{NO}_3^-$  versus  $\delta^{15}\text{N-NO}_3$  and  $\delta^{18}\text{O-NO}_3$ , respectively in the dry and  
442 wet seasons. The  $\delta^{15}\text{N-NO}_3$  and  $\delta^{18}\text{O-NO}_3$  values of water samples showed only weak correlations with  
443 the inverse  $\text{NO}_3^-$  concentrations ( $R^2 = 0.005$ ,  $p > 0.05$  and  $R^2 = 0.35$ ,  $p < 0.05$ ) and ( $R^2 = 0.012$ ,  $p > 0.05$   
444 and  $R^2 = 0.035$ ,  $p > 0.05$ ) in the dry and wet seasons, respectively. The plots for water samples exhibited  
445 that  $\delta^{15}\text{N-NO}_3$  and  $\delta^{18}\text{O-NO}_3$  were negatively correlated with  $1/[\text{NO}_3^-]$  confirming the limitation of  
446 denitrification processes in the Kabul aquifer. Weak negative relationships (Fig 8a-b) could be explained  
447 as the mixing of various nitrate sources such as sewage with soil organic nitrogen and chemical fertilizer  
448 (Romanelli et al., 2020). Overall, the data suggested that denitrification did not significantly influence the  
449 nitrate dynamics in the Kabul aquifer in the dry and wet seasons.

450

### 451 *3.7. Quantification of the dominant sources of nitrate by SIMMR model*

452 In order to quantitatively estimate the proportional contributions of various potential nitrate sources to the  
453 Kabul Plain, the Bayesian stable isotope mixing model (SIMM) in R with the SIMMR package was  
454 employed. Two isotopes ( $J=2$ ) ( $\delta^{15}\text{N-NO}_3$  and  $\delta^{18}\text{O-NO}_3$ ) and three potential sources of nitrate ( $K=3$ )  
455 (sewage and manure (S&M), soil organic N (SN) and chemical fertilizers (CF)) were employed. In this  
456 study, denitrification is not thought to have a major impact on the isotopic composition of  $\text{NO}_3^-$ , thus the  
457 fractionation factor is considered zero (Fadhullah et al., 2019; Zhang et al., 2020). According to the  
458 SIMMR, the contributions of the three potential  $\text{NO}_3^-$  sources were quantified, suggesting a considerable  
459 variability in the different seasons and areas (Table S1 and Fig. 9a and 9b). The  $\delta^{15}\text{N-NO}_3$  and  $\delta^{18}\text{O-NO}_3$   
460 values of the nitrate sources were based on the relevant literatures (Xue et al., 2009; Nikolenko et al.,  
461 2018; Torres-Martínez et al., 2020). Based on the SIMMR output results, sewage had the highest  
462 contribution (~81%), followed by soil organic nitrogen (10.5%), and chemical fertilizer (8.5%) in the dry

463 season. In the wet season, sewage (~87.5%), soil organic N (6.7%), and chemical fertilizer (5.8%)  
464 contributed in a similar proportion to the nitrate pool in the Kabul aquifer. The SIMMR results suggest  
465 that sewage was the dominant source of NO<sub>3</sub> in the Kabul aquifer. It reflects the influence of rapid  
466 urbanization in the Kabul Plain. The contribution of NO<sub>3</sub> from urban sewage to the Kabul aquifer is  
467 expected to increase due to the growing population, lack of sewerage collection system and wastewater  
468 treatment plants in the city. The sources of NO<sub>3</sub> estimated by SIMMR were quite reasonable and in good  
469 agreement with qualitative analysis of dual nitrate isotopes of nitrate and in-situ observations.

#### 470 **4. Conclusion**

471 An integrated approach that combined hydrogeochemical data, stable isotope signatures of nitrate and  
472 water, and a stable isotope mixing model (SIMMR) were employed to determine potential sources of  
473 nitrate, biogeochemical processes and seasonally proportional contributions of nitrate sources in the  
474 Kabul aquifer. The results indicated that NO<sub>3</sub> concentrations in the Kabul aquifer varied from place to  
475 place in urban land use and were significantly influenced by localized anthropogenic activities. The  
476 results of water stable isotope analyses indicated that rainfall and river water after evaporation were the  
477 major source of groundwater in the Kabul Plain. The dual stable isotope signatures of nitrate revealed that  
478 nitrification of sewage and human wastes was the main nitrate pollution source in the aquifer, which was  
479 confirmed by hydrogeochemical data. Nitrification was identified as a main biogeochemical process in  
480 the aquifer. The spatio-temporal variability in the proportional contribution of nitrate sources was  
481 determined by a Bayesian stable isotope mixing model (SIMMR). In this respect, sewage was the main  
482 contributor of groundwater nitrate in the Kabul aquifer in the dry and wet seasons followed by soil  
483 organic nitrogen and chemical fertilizers. This is the first detailed nitrate pollution study in Afghanistan  
484 employing an integrated approach. The combined approach of isotopic the composition of nitrate,  
485 hydrochemical and land use data and SIMMR model allowed a more reliable assessment of the nitrate  
486 sources, biogeochemical processes and nitrate source apportionment in groundwater of the Kabul aquifer.  
487 Continuous rehabilitation of existing sewerage collection systems and constructing decentralized on-site

488 treatment systems in new townships are important ways to reduce NO<sub>3</sub> pollution in the Kabul aquifer. A  
489 long-term monitoring of groundwater quality in the Kabul aquifer is strongly advised.

490

491 **CRedit authorship contribution statement**

492 **Abdulhalim Zaryab:** Conceptualization, Methodology, Investigation, Software, Data curation, Formal  
493 analysis, Writing – original draft, Writing – reviewing & editing, Visualization. **Hamid Reza Nassery:**  
494 Conceptualization, Methodology, Formal analysis, Supervision, Validation, Writing – reviewing &  
495 editing. **Kay Knoeller:** Conceptualization, Methodology, Resources, Supervision, Validation, Writing –  
496 reviewing & editing. **Farshad Alijani:** Conceptualization, Methodology, Software, Formal analysis,  
497 Visualization, Validation, Writing – reviewing and editing. **Eddy Minet:** Conceptualization,  
498 Methodology, Visualization, Validation, Writing – reviewing and editing.

499

500 **Conflict of Interest:** The authors declare no conflict of interest.

501

502 **Acknowledgement**

503 All the authors would like to thank Kabul Polytechnic University, Kabul, Afghanistan for providing field  
504 measurement equipment.

505

506 **Appendix:** Supplementary material

507

508 **References**

509 Anderson, K.K., Hooper, A.B., 1983. O<sub>2</sub> and H<sub>2</sub>O are each the source of one O in NO<sub>2</sub> produced from NH<sub>3</sub> by  
510 Nitrosomonas: 15N evidence. FEBS Lett. 164, 236-240.  
511 Aravena, R., Robertson, W.D., 1998. Using of Multiple isotope tracers to evaluate denitrification in  
512 groundwater: study of nitrate from a large-flux septic system plume. Groundwater, 36, 975-982.

513 Biddau, R., Cidu, R., Pelo, S.D., Carletti, A., Ghiglieri, G., Pittalis, D., 2019. Source and fate of nitrate in  
514 contaminated groundwater systems: assessing spatial and temporal variations by hydrogeochemistry and  
515 multiple stable isotope tools. *Sci. Total Environ.* 647, 1121-1136.  
516 <https://doi.org/10.1016/j.scitotenv.2018.08.007>.

517 Blarasin, M., Cabrera, A., Matiatos, I., Becher Quinodóz, F., Giuliano Albo, J., Lutri, V., Matteoda, E.,  
518 Panarello H., 2020. Comparative evaluation of urban versus agricultural nitrate sources and sinks in an  
519 unconfined aquifer by isotopic and multivariate analyses. *Sci. Total Environ.* 741, 140374.  
520 <https://doi.org/10.1016/j.scitotenv.2020.140374>.

521 Böttcher, J., Strebel, O., Voerkelius, S., Schmidt, H.-L., 1990. Using isotope fractionation of nitrate-nitrogen  
522 and nitrate-oxygen for evaluation of microbial denitrification in a sandy aquifer. *J. Hydrol.* 114, 413-424.

523 Broshears, R.E., Akbari, M.A., Chornack, M.P., Mueller, D.K., Ruddy, B.C., 2005. Inventory of groundwater  
524 resources in the Kabul Basin, Afghanistan: U.S. Geological Survey, Scientific Investigation Report 2005-5090,  
525 U.S. Geological Survey.

526 Casciotti, K.L., Buchwald, C., 2012. Insights on the marine microbial cycle from isotopic approaches to  
527 nitrification. In *Frontiers in microbiology* 3, p. 356. DOI: 10.3389/fmicb.2012.00356.

528 Casciotti, K.L., Sigman, D.M., Hastings, M.G., Böhlke, J.K., Hilkert, A., 2002. Measurement of the oxygen  
529 isotopic composition of nitrate seawater and freshwater using the denitrifier method. *Anal. Chem.* 74(19),  
530 4905-4912. <https://doi.org/10.1021/ac020113w>.

531 Cey, E.E., Rudolph, D.I., Aravena, R., Parkin, G., 1999. Role of the riparian zone in controlling the  
532 distribution and fate of agricultural nitrogen near a small stream in southern Ontario. *J. Contam. Hydrol.* 37,  
533 45-67.

534 Cheng, C.C.Y., Kendall, C., Silva, S.R., Battaglin, W.A., Campbell, D.H., 2002. Nitrate stable isotopes: tools  
535 for determining nitrate sources among different land uses in the Mississippi River Basin. *Can. J. Fish. Aquat.*  
536 *Sci.* 59, 1874-1885. Doi: 10.1139/f02-153.

537 Clark, I., Fritz, P., 1997. *Environmental Isotopes in Hydrogeology*. CRC Press, New York.

538 Clark, I., 2015. *Groundwater Geochemistry and Isotopes*. CRC Press/Taylor & Francis. Group, Boca  
539 Raton/London/New York, 438 pages.

540 Cook, P.G., 2013. Estimating groundwater discharge to rivers from river chemistry surveys. *Hydrol. Processes*.  
541 27(25), 3694-3707. <https://doi.org/10.1002/hyp.9493>.

542 Dansgaard, W., 1964. Stable isotopes in precipitation. *Tellus*, 16(4), 436-468. <https://doi.org/10.1111/j.2153->  
543 [3490.1964.tb00181.x](https://doi.org/10.1111/j.2153-3490.1964.tb00181.x)

544 Das, P., Mukherjee, A., Hussain, S.A., Jamal, M.S., Das, K., Show, A., Layek, M.K., Sengupta, P., 2020.  
545 Stable isotope dynamics of groundwater interactions with Ganges River. *Hydrol. Processes*. 35, e14002.  
546 <https://doi.org/10.1002/hyp.14002>.

547 Ding, J., Xi, B., Gao, R., He, L., Liu, H., Dai, X., Yu, Y., 2014. Identifying diffused nitrate sources in a  
548 stream in an agricultural field using a dual isotopic approach. *Sci. Total Environ*. 484, 10-18.  
549 <http://dx.doi.org/10.1016/j.scitotenv.2014.03.018>.

550 Deutsch, B., Mewes, M., Liskow, I., Voss, M., 2006. Quantification of diffuse nitrate inputs into a small river  
551 system using stable isotopes of oxygen and nitrogen in nitrate. *Org, Chem*. 37, 1333-1342. DOI:  
552 10.1016/j.orggeochem.2006.04.012.

553 Domenico, P.A., Schwartz, F.W., 1990. *Physical and chemical hydrogeology*. John Wiley & Sons. Inc. 824 p.

554 Exner-Kittredge, M., Strauss, P., Bloschl, G., Eder, A., Saracevic, E., Zessner, M., 2016. The seasonal dynamics  
555 of the stream sources and input flow paths of water and nitrogen of an Austrian headwater agricultural  
556 catchment. *Sci. Total Environ*. 542, 935-945. <http://dx.doi.org/10.1016/j.scitotenv.2015.10.151>.

557 Fadhullah, W., Yaccob, N. S., Syakir, M. I., Muhammad, S. A., Yue, F. J. & Li, S. L., 2020. Nitrate sources  
558 and processes in the surface water of a tropical reservoir by stable isotopes and mixing model. *Sci. Total*  
559 *Environ*. 700, 134517. <https://doi.org/10.1016/j.scitotenv.2019.134517>.

560 Fan, A.M., and Steinberg, V.E., 1996. Health implications of nitrate and nitrate in drinking water: an update on  
561 methemoglobinemia occurrence and reproductive and developmental toxicity. *Regul. Toxicol. Pharmacol*. 23,  
562 35-43.

563 Fewtrell, L., 2004. Drinking-water nitrate, methemoglobinemia, and global burden of disease: a discussion.  
564 *Environ. Health Perspect*. 112, 1371-1374.

565 Gat, J.R., Carmi, I., 1970. Evolution of the isotopic composition of atmospheric waters in the Mediterranean  
566 Sea Area. *J. Geophys. Res*. 75(15): 3039-3048.

567 Griffiths, N.A., Jackson, C.R., McDonnell, J.J., Klaus, J., Du, E., Bitew, M.M., 2016. Dual nitrate isotopes  
568 clarify role of biological processing and hydrologic flow paths on nitrogen cycling in subtropical low-gradient  
569 watersheds. *J. Geophys. Res. Biogeosci.*, 121, 422-437. DOI: 10.1002/2015JG003189.

570 Gulis, G., Czompolyova, M., Cerhan J.R., 2002. An ecologic study of nitrate in municipal drinking water and  
571 cancer incidence in Trnava district, Slovakia. *Environ. Res. Sec. A.* 88, 182-187.

572 Herms, I., Jodár, J., Soler, A., Lambán L.J., Custodio, E., Nùñez, J.A., Arnó, G., Parcerisa, D., Jorge-Sánchez  
573 J., 2021. Identification of natural and anthropogenic geochemical processes determining the groundwater  
574 quality in Port del Comte High Mountain karst aquifer (SE, Pyrenees). *Water*, 13, 2891.  
575 <https://doi.org/10.3390/w13202891>

576 Hocaoglu, S.M., Insel, G., Cokgor, E.U., Orhon, D., 2011. Effect of sludge age on simultaneous nitrification  
577 and denitrification in membrane. *Bioresour. Technol.* 102, 6665-6672. DOI: 10.1016/j.biortech.2011.03.096.

578 Houben G, Tunnermeier T, Himmelsbach T., 2005. Hydrogeology of the Kabul Basin- Part II: Groundwater  
579 Geochemistry and Microbiology. Foreign Office of the Federal Republic of Germany, BGR.

580 Houben G, Tünnermeier T, Eqrar N., 2008. Hydrogeology of the Kabul Basin (Afghanistan), part II:  
581 groundwater chemistry, *Hydrogeol. J.* 17(4):935-948. DOI: 10.1007/s10040-008-0375-1.

582 Houben G, Niard N, Tunnermeier T Himmelsbach T. 2009. Hydrogeology of the Kabul Basin (Afghanistan),  
583 part 1: aquifer and hydrology. *Hydrogeol. J.* 17(3):665-677. <https://doi.org/10.1007/s10040-008-0377-z>.

584 Jin, Z., Cen, J., Hu, J., Li, L., Shi, Y., Fu, G., Li, F., 2019. Quantifying nitrate sources in a large reservoir for  
585 drinking water by using stable isotopes and a Bayesian isotope mixing model. *Environ. Sci. Pollut. Res.* 26,  
586 20364-20376. <https://doi.org/10.1007/s11356-019-05296-7>.

587 Kaushal, S.S., Groffman, P.M., Band, L.E., Elliot, E.M., Shields, C.A., Kendall, C., 2011. Tracing nonpoint  
588 source nitrogen population in human-impacted watersheds. *Environ. Sci. Technol.* 45, 8225-8232,  
589 <https://doi.org/10.1021/es200779e>.

590 Kendall, C., 1998. Tracing nitrogen sources and cycling in catchments. In: Kendall, C., McoDonnell, J.H.  
591 (Eds), *Isotope Tracers in Catchment Hydrology*. Elsevier, Amsterdam.

592 Kendall, C., Elliot, E.M., Wankel, S.D., 2007. Tracing anthropogenic inputs of nitrogen to ecosystems,  
593 chapter 12. In: Michener, R.H., Lajtha, K. (Eds.), *Stable Isotopes in Ecology and Environmental Science*, 2ed,  
594 edn Blackwell Publishing, pp. 375-449.

595 Kim, H., Kaown, D., Mayer, B., Lee, J.-Y., Hyun, Y., Lee, K.-K., 2015. Identifying the sources of nitrate  
596 contamination of groundwater in an agricultural area (Haean basin Korea) using isotope and microbial  
597 community analyses. *Sci. Total Environ.* 533, 566-575. <http://dx.doi.org/10.1016/j.scitotenv.2015.06.080>.

598 Kool, D.M., Warge, N., Oenema, O., Van Kessel, C., Van Groenigen, J.W., 2011. Oxygen exchange with  
599 water alters the oxygen isotopic signature of nitrate in soil ecosystems. *Soil Biol. Biochem.* 43 (6), 1180-1185.  
600 <https://doi.org/10.1016/j.soilbio.2011.02.006>.

601 Korth, E., Deutsch, B., Frey, C., Moros, C., Voss, M., 2014. Nitrate source identification in the Baltic Sea  
602 using its isotopic ratios in combination with a Bayesian isotope mixing model. *Biogeosciences*, 11, 4913-4924.  
603 DOI: 10.5194/bg-11-4913-2014.

604 Landell Mills. 2020. Regional Groundwater Model. TA 8969 AFG: Kabul Managed Aquifer Recharge Project  
605 Preparation, Kabul: Landell Mills.

606 Li, C., Li, S.-L., Yue, F.-J., Liu, J., Zhong, J., Yan, Z.-F., Zheng, R.-C., Wang, Z.-J., Xu, S., 2019.  
607 Identification of sources and transformations of nitrate in the Xijiang River using nitrate isotopes and Bayesian  
608 model. *Sci. Total Environ.* 646, 801-810. <https://doi.org/10.1016/j.scitotenv.2018.07.345>.

609 Liu, T., Wang, F., Michalski, G., Xia, X., Liu, S., 2013. Using  $^{15}\text{N}$ ,  $^{17}\text{O}$ , and  $^{18}\text{O}$  to determine nitrate sources in  
610 the Yellow River, China. *Environ. Sci. Technol.* 47, 13412-13421. <http://dx.doi.org/10.1021/es403357m>

611 Luu, T.N.M., Do, T.N., Matiatos, I., Panizzo, V.N., Trinh, A.D., 2020. Stable isotopes as an effective tool for  
612 N nutrient sources identification in heavily urbanized and agriculturally intensive tropical lowland basin.  
613 *Biogeochemistry* <https://doi.org/10.1007/s10533-020-00663-3>.

614 Mack, T.J., Akbari, M.A., Ashoor, M.H., Chornack, M.P., Coplen, T.B., Emerson, D.D., et al., 2010.  
615 Conceptual model of water resources in the Kabul Basin, Afghanistan. U.S. Geological Survey scientific  
616 investigations report 2009-5262.

617 Matiatos, I., 2016. Nitrate source identification in groundwater of multiple land-use areas by combining  
618 isotopes and multivariate statistical analysis: a case study of Asopos basin (Central Greece). *Sci. Total*  
619 *Environ.* 541, 802-814. <http://dx.doi.org/10.1016/j.scitotenv.2015.09.134>.

620 Mayer, B., Boyer, B.W., Goodale, C., Jaworski, N.A., Breemen, N.V., Howarth, R.W., et al., 2002. Source of  
621 nitrate in rivers draining sixteen watersheds in the northeastern U.S. isotopic constraint. *Biogeochemistry* 57,  
622 171-197. <https://doi.org/10.1023/A:1015744002496>.

623 Meghdadi, A., Javar, N., 2018, Quantification of spatial and seasonal variations in the proportional  
624 contribution of nitrate sources using a multi-isotope approach and Bayesian isotope mixing model. *Environ.*  
625 *Pollut.* 235, 207-222. <https://doi.org/10.1016/j.envpol.2017.12.078>.

626 Meldebekova, G., Yu, C, Li, Z., Song, C., 2020. Quantifying groundwater subsidence associated with aquifer  
627 overexploitation using space-borne radar interferometry in Kabul, Afghanistan. *Remote Sens.* 12, 2461.  
628 <https://doi.org/10.3390/rs12152461>.

629 Minet, E.P., Goodhue, R., Meier-Augenstein, W., Kalin, R.M., Fenton, O., Richards, K.G., Coxon, C.E., 2017.  
630 Combining stable isotopes with contamination indicators: a method for improved investigation of nitrate  
631 sources and dynamics in aquifers with mixed nitrogen inputs. *Water Res.* 124, 85-96.  
632 <https://doi.org/10.1016/j.watres.2017.07.041>.

633 Mingming, H., Yuchun, W., Pengcheng, D., Yong, Aimin, C., Cong, L., Yufei, B., Yanhui, L., Shanze, L.,  
634 Panwei, Z., 2019. Tracing the sources of nitrate in the rivers and lakes of the southern areas of the Tibetan  
635 Plateau using dual nitrate isotopes. *Sci. Total Environ.* 658, 132-140.  
636 <https://doi.org/10.1016/j.scitotenv.2018.12.149>.

637 Mook, W.G., De Vries, J.J., 2000. Environmental isotope in the hydrological cycle, principle and application,  
638 vol.1. Theory, Methods, Review. Accessible at: [Environmental isotopes in the hydrological cycle: Principles and](https://www.hydrology.nl/en/publications-and-reports/publications/Environmental-isotopes-in-the-hydrological-cycle-Principles-and-applications)  
639 [applications • Hydrology.nl](https://www.hydrology.nl/en/publications-and-reports/publications/Environmental-isotopes-in-the-hydrological-cycle-Principles-and-applications)

640 Nejatijahromi, Z., Nassery, H.R., Hosono, T., Nakhaei, M., Alijani, F., Okumura, A., 2019. Groundwater  
641 nitrate contamination in an area using urban wastewaters for agricultural irrigation under arid climate  
642 condition, southeast of Tehran, Iran. *Agric. Water Manag.* 221:397–414. DOI: 10.1016/j.agwat.2019.04.015.

643 Nestler, A., Berglund, M., Accoe, F., Duta, S., Xue, D., Boeckx, P., Taylor, P., 2011. Isotopes for improved  
644 management of nitrate pollution in aqueous resources: review of surface water field studies. *Environ. Sci.*  
645 *Pollut. Res.* 18, 519-533. DOI: 10.1007/s11356-010-0422-z.

646 Nikolenko, O., Jurado, A., Borges, A.V., Knöller, K., Brouyère, S., 2017. Isotopic composition of nitrogen  
647 species in groundwater under agricultural areas: A review, *Sci. Total Environ.*  
648 <https://doi.org/10.1016/j.scitotenv.2017.10.086>.

649 Ogrinc, N., Tamše, S., Zavadlav, S., Vrzel, J., Jin, L., 2019. Evaluation of geochemical processes and nitrate  
650 pollution sources at the Ljubljansko polje aquifer (Slovenia): A stable isotope perspective. *Sci. Total Environ.*  
651 646, 1588-1600. <https://doi.org/10.1016/j.scitotenv.2018.07.245>.

652 Paiman, Z., Noori, A. R., 2019. Evaluation of wastewater collection and disposal in Kabul city and its  
653 environmental impacts. *Modern Environ. Sci. Eng.* 5(5), 451-458. DOI: 10.15341/mese(2333-  
654 2581)/05.05.2019/012.

655 Panno, S.V., Hackley, K.C., Kelly, W.R., Hwang, H.H., 2006. Isotopic evidence of nitrate sources and  
656 denitrification in the Mississippi River, Illinois. *J. Environ. Qual.* 35(2), 495-504.

657 Parnell, A.C., Inger, R., Bearhop, S., Jackson, A.L., 2010. Source partitioning using stable isotopes: with too  
658 much variation. *PloS ONE* 5(3): e9672. DOI: 10.1371/journal.pone.0009672.

659 Parnell, A.C., Phillips, D.L., Bearhop, S., Semmens, B.X., Ward, E.J., Moore, J.W., Jackson, A.L., Grey,  
660 J., Kelly, D.J., Inger, D.J., 2013. Bayesian stable isotope mixing models. *Environmetrics* 24(6), 387-399.  
661 <https://doi.org/10.1002/env.2221>

662 Parnell, A.C., Inger, R., 2016. Simmr: A stable isotope mixing model. R Package version 0.4.1.

663 Pastén-Zapata, E., Ledesma-Ruiz, R., Harter, T., Ramirez, A.I., Mählknecht, J., 2014. Assessment of sources  
664 and fate of nitrate in shallow groundwater of an agricultural area by using a multi-tracer approach. *Sci. Total*  
665 *Environ.* 470/471, 855-864. <http://dx.doi.org/10.1016/j.scitotenv.2013.10.043>.

666 Phillips, D., Koch, P.L., 2002. Incorporating concentration dependence in stable isotope mixing models.  
667 *Oecologia*, 130, 114-125. DOI: 10.1007/s004420100786.

668 Popescu, R., Mimmo, T., Dinca, O.R., Capici, C., Costinel, D., Sandru, C., Ionete, R.E., Stefanescu, I., Axente,  
669 D., 2015. Using stable isotopes in tracing contaminant sources in an industrial area: A case study on the

670 hydrological basin of the Olt River, Romania, *Sci. Total Environ.* 533, 17-23.  
671 <http://dx.doi.org/10.1016/j.scitotenv.2015.06.078>.

672 Re, V., Kammoun, S., Sacchi, E., Trabelsi, R., Zouari, K., Matiatos, I., Allais, E., Daniele, S., 2021. Acritical  
673 assessment of widely used techniques for nitrate source apportionment in arid and semi-arid regions. *Sci. Total*  
674 *Environ.* 775, 145688. <https://doi.org/10.1016/j.scitotenv.2021.145688>.

675 Rivett, M.O., Buss, S.R., Morgan, P., Smith, J.W.N., Bemment, C.D., 2008. Nitrate attenuation in  
676 groundwater: a review of biogeochemical controlling processes. *Water Res.* 42, 4215-4232. DOI:  
677 10.1016/j.watres.2008.07.020.

678 Romanelli, A., Soto, D.X., Matiatos, I., Martínez D.E., Esquiús, S., 2020. A biological and nitrate isotopic  
679 assessment framework to understand eutrophication in aquatic ecosystems. *Sci. Total Environ.* 715, 136909.  
680 <https://doi.org/10.1016/j.scitotenv.2020.136909>.

681 Rozanski, K., Araguas-Araguas, L., Gofiantini, R., 1993. Isotopic patterns in modern global precipitation, in  
682 climate change in continental isotope records. *Geophys. Monogr. Ser.* 78, 1-36.

683 Safi, Z., Bahram, G.M., Alemi, M.A., 2017. Organic matter and nutrient losses via runoff (March/December,  
684 2016) in urban agriculture of Kabul, Afghanistan. *IJARR* 5(2): 588-597.

685 Savard, M.M., Somers, G., Smirnoff, A., Paradis, D., Bochove, E.V., Liao, S., 2009. Nitrate isotopes unveil  
686 distinct seasonal-N-sources and the critical role of crop residues in groundwater contamination. *J. Hydrol.*  
687 doi:10.1016/j.jhydrol.2009.11.033.

688 Sebestyen, S.D., Ross, D.S., Shanley, J.B., Elliott, E.M. et al., 2019. Unprocessed atmospheric nitrate in waters  
689 of the Northern Frost Region in the U.S. and Canada. *Environ. Sci. Technol.* 53, 3620-3633. DOI:  
690 10.1021/acs.est.9b01276.

691 Shalev, N., Burg, A., Gavrieli, I., Lazar, B., 2015. Nitrate contamination sources in aquifers underlying  
692 cultivated fields in an arid region- The Arava Valley, Israel. *Appl. Geochem.* 63, 322-332.  
693 <https://doi.org/10.1016/j.apgeochem.2015.09.017>.

694 Sigman, D.M., Casciotti, K.L., Andreani, M., Barford, C., Galanter, M., Böhlke, J.K., 2001. A bacterial  
695 method for the nitrogen isotopic analysis of nitrate in seawater and freshwater. *Anal. Chem.* 73(17), 4145-  
696 4153. <https://doi.org/10.1021/ac10088e>.

697 Soto, D.X., Koehler, G., Wassenaar, L.I., Hobson, K.A., 2019. Spatio-temporal variation of nitrate sources to  
698 Lake Winnipeg using N and O isotope ( $\delta^{15}\text{N}$  and  $\delta^{18}\text{O}$ ) analyses. *Sci. Total Environ.* 647, 486-493.  
699 <https://doi.org/10.1016/j.scitotenv.2018.07.346>.

700 Suchy, M., Wassenaar, L.I., Graham, G., Zebarth, B., 2018. High-frequency of  $\text{NO}_3^-$  isotope ( $\delta^{15}\text{N}$  and  $\delta^{18}\text{O}$ )  
701 pattern in groundwater recharge reveal that short-term changes in land use and precipitation influence nitrate  
702 contamination trends. *Hydro. Earth Syst. Sci.* 22, 4267-4279. <https://doi.org/10.5194/hess-22-4267-2018>.

703 Torres-Martínez, J.A., Mora, A., Knappett, P.S.K., Ornelas-Soto, N., Mahlkecht, J., 2020. Tracking nitrate  
704 and sulfate source in groundwater of an urbanized valley using a multi-tracer approach combined with a  
705 Bayesian isotope mixing model. *Water Res.* 182, 115962. <https://doi.org/10.1016/j.watres.2020.115962>.

706 Torres-Mrtínez J.A., Mora, A., Mahlkecht, J., Kaown, D., Barceló., 2021. Determining nitrate and sulfate  
707 pollution sources and transformations in a coastal aquifer impacted by seawater intrusion-A multi-isotopic  
708 approach combined with self-organized maps and a Bayesian mixing model. *J. Hazard. Mater.* 417, 126103.  
709 <https://doi.org/10.1016/j.jhazmat.2021.126103>.

710 Utom, A.U., Werban, U., Levan, C., Muller, C., Knoller, K., Vogt, C., Dietrich, P., 2020. Groundwater  
711 nitrification and denitrification are not always strictly aerobic and anaerobic processes, respectively: an  
712 assessment of dual-nitrate isotopic and chemical evidence in a stratified alluvial aquifer: Biogeochemistry  
713 147, 211-223. <https://doi.org/10.1007/s10533-020-00637-y>.

714 Voss, M., Deutsh, B., Elmgren, R., Humborg, C., Kuuppo, P., Pastuszak, M., Roff, C., Schulte, U., 2006.  
715 Source identification of nitrate by means of isotopic tracers in the Baltic Sea catchments. *Biogeosciences* 3,  
716 663-676. [www.biogeosciences.net/3/663/2006/](http://www.biogeosciences.net/3/663/2006/).

717 Ward, M.H., deKok, and Levallois, P., 2005. Workgroup report: drinking-water nitrate and health-recent  
718 findings and research needs. *Environ. Health Perspect.* 113, 1607-1614.v

719 Wassenaar, L., 1995. Evaluation of origin and fate of nitrate in the Abbotsford Aquifer using the isotopes of  
720  $^{15}\text{N}$  and  $^{18}\text{O}$  in  $\text{NO}_3^-$ . *Appl. Geochemistry.* 10, 391-405.

721 Weitzman, J.N., Brooks, J.R., Mayer, M.P., Rugh, W.D., Compton, J.E., 2021. Coupling the dual isotopes of  
722 water ( $\delta^2\text{H}$  and  $\delta^{18}\text{O}$ ) nitrate ( $\delta^{15}\text{N}$  and  $\delta^{18}\text{O}$ ): a new framework for classifying current and legacy groundwater  
723 pollution. *Environ. Res. Lett.* 16, 045008. <https://doi.org/10.1088/1748-9326/abdcef>.

724 Wexler, S.K., Hiscock, K.M., Dennis, P.F., 2012. Microbial and hydrological influences on nitrate isotopic  
725 composition in an agricultural lowland catchment. *J. Hydrol.* 468, 85-93.  
726 <https://doi.org/10.1016/j.jhydrol.2012.08.018>.

727 WHO, (World Health Organization), 2017. *Guideline for Drinking-Water Quality: Fourth Edition*  
728 *Incorporating the First Addendum*, fourth ed. Geneva. [https://doi.org/10.1016/S1462-0758\(00\)00006-6](https://doi.org/10.1016/S1462-0758(00)00006-6).

729 Widory, D., Petelet-Giraud, E., Brenot, A., Bronders, J., Tirez, K., Boeckx, P., 2013. Improving the  
730 management of nitrate pollution in water by the use of isotope monitoring: the  $\delta^{15}\text{N}$ ,  $\delta^{18}\text{O}$  and  $\delta^{11}\text{B}$  triptych.  
731 *Iso Environ. Health Stud.* 49 (1), 29-47. <https://doi.org/10.1080/10256016.2012.666540>.

732 World Health Organization, 2017. *Guidelines for Drinking-water Quality; 4<sup>th</sup> Edition, Incorporating the 1<sup>st</sup>*  
733 *Addendum*.

734 Wu, H., Dong, Y., Gao, L., Song, X., Liu, F., Peng, X., Zhang, G.-L., 2020. Identifying nitrate sources in  
735 surface water, regolith and groundwater in a subtropical red soil Critical Zone by using dual isotopes.  
736 *CATENA.* 198, 104994.

737 Xue, D., Bottle, J., Baets, B., Accoe, F., Nestler, A., Taylor, P., Cleemput, O., Berglund, M., Boeckx, P., 2009.  
738 Present limitations and future prospects of stable isotopes methods for nitrate source identification in surface  
739 and groundwater. *Water Res.* 43, 1159-1170.

740 Xue, D., Baets, B.D., Cleemput, O.V., Hennessy, C., Berglund, M., Boeckx, P., 2012. Use of a Bayesian  
741 isotope mixing model to estimate proportional contributions of multiple nitrate sources in surface water.  
742 *Environ. Pollut.* 161, 43-49. DOI: 10.1016/j.envpol.2011.09.033.

743 Xu, S., Kang, P., Sun, Y., 2016. A stable isotope approach and its application for identifying nitrate source and  
744 transformation process in water. *Environ. Sci. Pollut. Res.* 23, 1133-1148. DOI: 10.1007/s11356-015-5309-6.

745 Yang, P., Wang, Y., Wu, X., Chang, L., Ham, B., Song, L., Groves, C., 2020. Nitrate source and  
746 biogeochemical processes in karst underground rivers impacted by different anthropogenic input  
747 characteristics. *Environ. Pollut.* 265, 114835. <https://doi.org/10.1016/j.envpol.2020.114835>.

748 Yang, Y.-Y., Toor, G.S., 2016.  $\delta^{15}\text{N}$  and  $\delta^{18}\text{O}$  reveal the source of nitrate-nitrogen in urban residential  
749 stormwater runoff. *Environ. Sci. Technol.* 50(6): 2881-2889. DOI: 10.1021/acs.est.5b05353.

750 Ye, H., Tang, C., Cao, Y., 2021. Sources and transformation mechanisms of inorganic nitrogen: Evidence from  
751 multi-isotopes in a rural-urban river area. *Sci. Total Environ.* 794, 148615.  
752 <https://doi.org/10.1016/j.scitotenv.2021.148615>.

753 Yi, Q., Chen, Q., Hu, L., Shi, W., 2017. Tracking nitrogen sources, transformation and transport at a basin  
754 scale with complex plain river networks. *Environ. Sci. Technol.* 51 (10), 5396-5403.

755 Yue, F.J., Liu, C.Q., Li, S.L., Zhao, Liu, X.L., Ding, H., Liu, B.J., Zhong, J., 2014. Analysis of  $\delta^{15}\text{N}$  and  $\delta^{18}\text{O}$   
756 to identify nitrate sources and transformations in Songhua River, Northeast China. *J. Hydrol.* 519, 329-339.  
757 <https://doi.org/10.1016/j.jhydrol.2014.07.026>.

758 Zaryab, A., Nassery, H.R., Alijani, F., 2021. Identifying sources of groundwater salinity and major  
759 hydrogeochemical processes in the Lower Kabul Basin aquifer, Afghanistan. *Environ. Sci.: Process. Impacts.*  
760 23, 1589-1599. <https://doi.org/10.1039/D1EM00262G>.

761 Zendeabad, M., Cepuder, P., Loiskandl, W., Stumpp, C., 2019. Source identification of nitrate contamination  
762 in the urban aquifer of Mashhad, Iran. *J. Hydrol. Reg. Stud.* 25, 100618.  
763 <https://doi.org/10.1016/j.ejrh.2019.100618>.

764 Zhang, Y., Shi, P., Li, F., Wei, L., Song, J., Ma, J., 2018. Quantification of nitrate sources and fates in rivers in  
765 an irrigated agricultural area using environmental isotopes and a Bayesian isotope mixing model.  
766 *Chemosphere*, 208: 493-501. DOI: [10.1016/j.chemosphere.2018.05.164](https://doi.org/10.1016/j.chemosphere.2018.05.164).

767 Zhang, H., Xu, Y., Cheng, S., Li, Q., Yu, Q., 2020. Application of the dual-isotope approach and Bayesian  
768 isotope mixing model to identify nitrate in groundwater of a multiple land-use area in Chengdu Plain, China.  
769 *Sci. Total Environ.* 717, 137134. <https://doi.org/10.1016/j.scitotenv.2020.137134>.

770 Zhao, Y., Zheng, B., Jia, H., Chen, Z., 2019. Determination sources of nitrate into the Three Gorges Reservoir  
771 using nitrogen and oxygen isotopes. *Sci, Total Environ.* 687, 128-136.  
772 <https://doi.org/10.1016/j.scitotenv.2019.06.073>.

773 Zheng, Y., Li, F., Zheng, Q., Li, J., Liu, Q., 2014. Tracing nitrate pollution sources and transformation in  
774 surface and groundwaters using environmental isotopes. *Sci. Total Environ.* 490, 213-222.  
775 <http://dx.doi.org/10.1016/j.scitotenv.2014.05.004>.

776 Zhu, A., Chen, J., Gao, L., Shimizu, Y., Liang, D., Yi, M., Cao, L., 2019. Combined microbial and isotopic  
 777 signature approach to identify nitrate sources and transformation processes in groundwater. *Chemosphere*, 228,  
 778 721-734. <https://doi.org/10.1016/j.chemosphere.2019.04.163>.

779

780

781

782

783

784

785

786

787

788

789

790

791

792

793

794

795

796

Table 1. Summary of  $\delta^{15}\text{N-NO}_3^-$ ,  $\delta^{18}\text{O-NO}_3^-$  isotopic signatures, from some possible end-members employed in the SIMMR model (Zhang et al., 2018; Torres-Mrtínez et al., 2020; Torres-Mrtínez et al., 2021)

Source	Dry season	Wet season	Dry season	Wet season
	$\delta^{15}\text{N-NO}_3^-$ Mean $\pm$ SD	$\delta^{18}\text{O-NO}_3^-$ Mean $\pm$ SD	$\delta^{15}\text{N-NO}_3^-$ Mean $\pm$ SD	$\delta^{18}\text{O-NO}_3^-$ Mean $\pm$ SD
Sewage and Manure (S&M)	12.20 $\pm$ 3.53	4.87 $\pm$ 1.87	13.2 $\pm$ 3.73	4.38 $\pm$ 3.72
Soil Organic Nitrogen (SN)	3.98 $\pm$ 1.95	2.51 $\pm$ 1.41	3.98 $\pm$ 1.82	2.47 $\pm$ 1.41
Chemical fertilizer (CF)	0.90 $\pm$ 2.00	2.80 $\pm$ 1.70	0.90 $\pm$ 2.0	2.60 $\pm$ 1.90

797

798

799

800

801

802

803

804

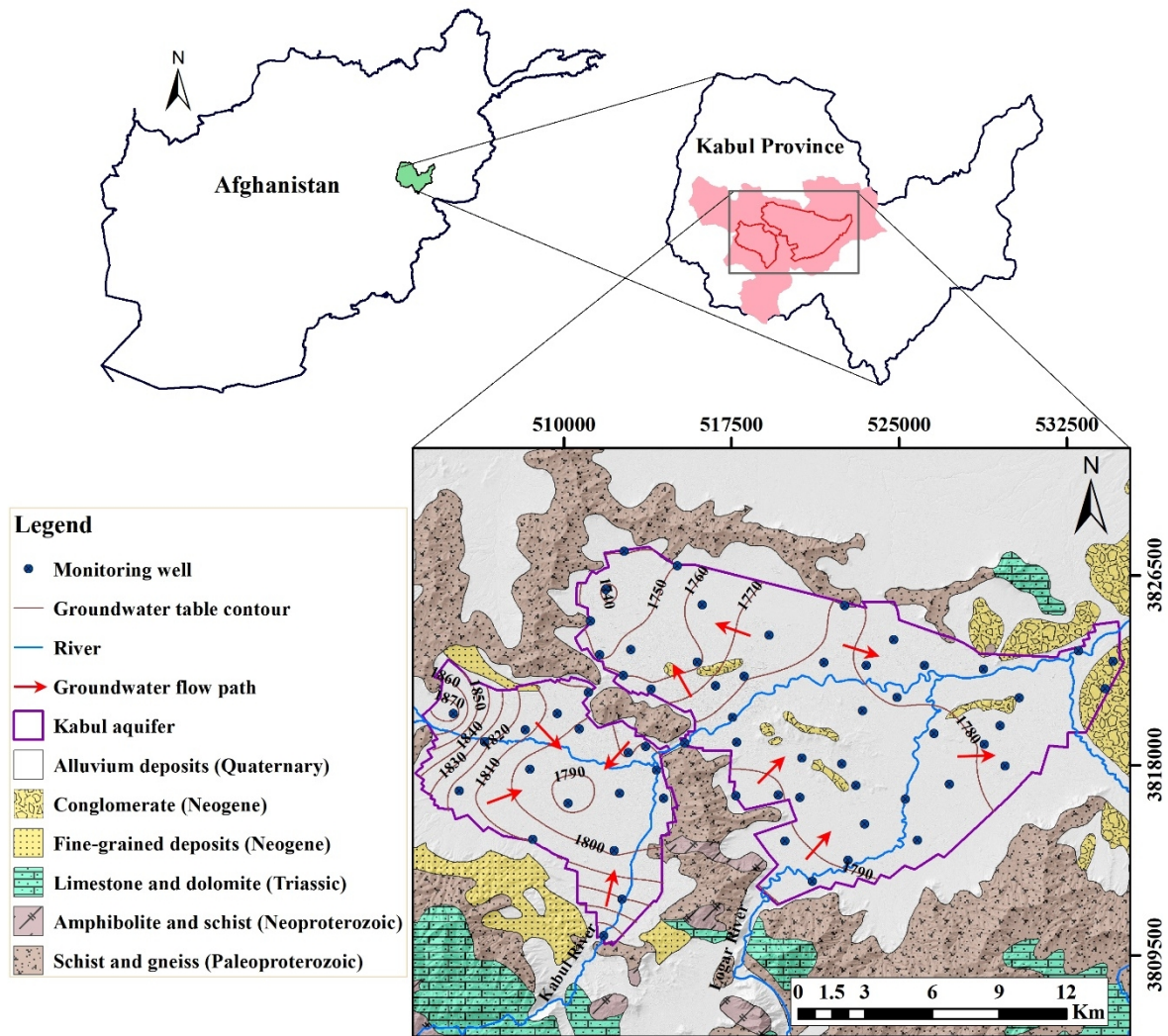
Table 2. Statistical summary of the physical, chemical, and isotopic results on sampling point in the Kabul Plain

Parameter	Unit	Dry season (November 2020)				Wet season (April 2021)			
		Min	Mean	Max	Std Dev	Min	Mean	Max	Std Dev
pH	-	7.00	7.60	8.10	0.23	7.10	5.26	8.30	1.59
T	°C	6.00	15.40	17.80	2.10	12.70	16.15	18.00	1.47
DO	mg/L	2.10	5.23	9.60	1.88	1.90	5.26	8.30	1.59
EC	$\mu\text{S/cm}$	618.0	1640.0	16400	3827.60	458.0	1429.50	16430	3653.90
Ca <sup>2+</sup>	mg/L	20.50	79.45	727.30	131.10	22.40	57.30	365.00	68.55
Mg <sup>2+</sup>	mg/L	12.30	82.40	738.00	153.10	11.40	57.00	520.20	130.60
Na <sup>+</sup>	mg/L	20.50	94.15	3014.0	672.85	15.56	71.68	2374.80	540.58
K <sup>+</sup>	mg/L	2.16	7.05	74.00	15.40	2.10	5.58	85.80	18.44
HCO <sub>3</sub> <sup>-</sup>	mg/L	183.0	429.9	840.0	170.60	183.0	393.45	802.76	163.87
Cl <sup>-</sup>	mg/L	7.30	135	3997	838.60	6.75	89.29	3163.40	622.77

SO <sub>4</sub> <sup>2+</sup>	mg/L	19.80	114	4573	1074.23	16.32	102.24	4582.10	955.85
NO <sub>3</sub> <sup>-</sup>	mg/L	3.98	13.7	120.41	21.30	4.87	17.71	58.88	13.24
NO <sub>2</sub> <sup>-</sup>	mg/L	0.01	0.20	2.80	0.55	0.01	0.03	0.36	0.11
δ <sup>15</sup> N-NO <sub>3</sub> <sup>-</sup>	‰AIR	4.80	10.20	20.80	3.98	6.90	12.00	25.40	4.28
δ <sup>18</sup> O-NO <sub>3</sub> <sup>-</sup>	‰VSMOW	-11.70	7.20	18.60	6.41	-3.40	4.00	11.50	3.55
δ <sup>2</sup> H-H <sub>2</sub> O	‰VSMOW					-73.40	-52.00	-30.30	7.67
δ <sup>18</sup> O-H <sub>2</sub> O	‰VSMOW					-10.59	-8.31	-6.39	0.90
NH <sub>4</sub> <sup>+</sup>	mg/L	0.01	0.04	53.05	9.83	0.00	0.60	109.80	63.09

805

806



807

808 **Fig. 1.** Location of Kabul aquifer with simplified geological map (Houben et al 2009; Bohannon 2010).

809 Groundwater table contours (August 2020) and flow directions (red arrows) are shown. The labeled

810 contour lines represent the elevation of the groundwater table.

812

813

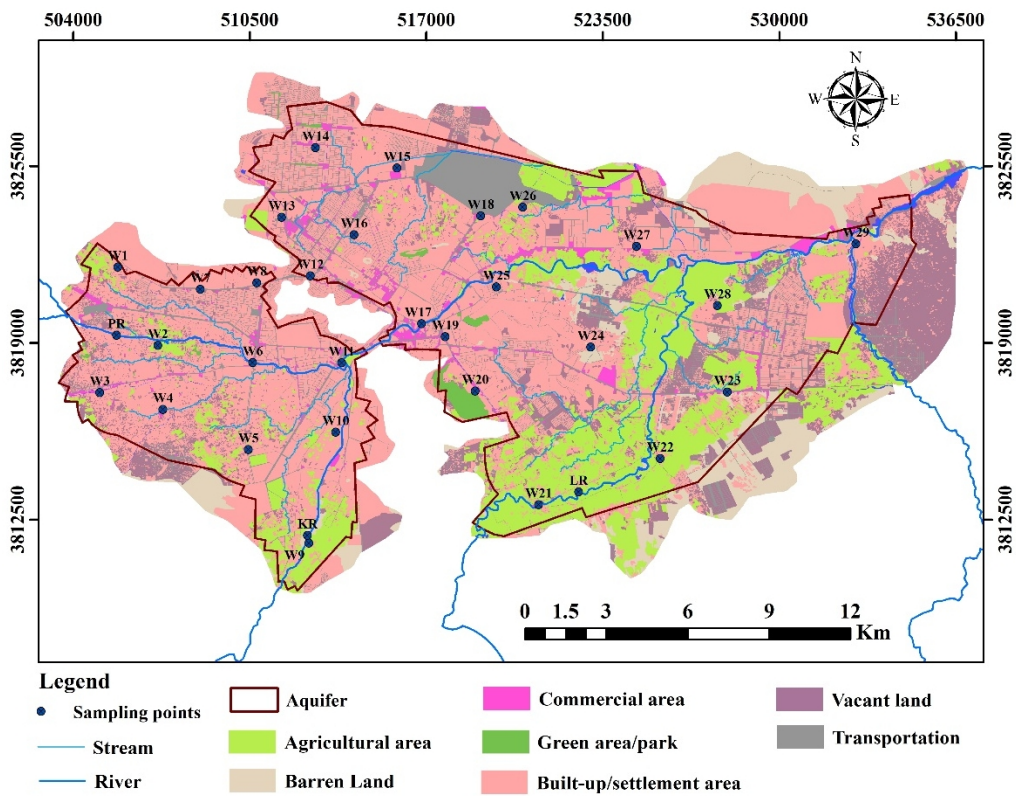


**Fig. 2.** Land use map of the study area (Kabul city, Afghanistan) and locations of sampling points.

814  
815  
816  
817  
818  
819  
820  
821  
822  
823  
824  
825  
826  
827  
828  
829  
830  
831  
832

833  
834  
835  
836  
837  
838  
839  
840  
841  
842  
843  
844  
845  
846  
847  
848  
849  
850  
851  
852  
853  
854  
855  
856  
857  
858  
859

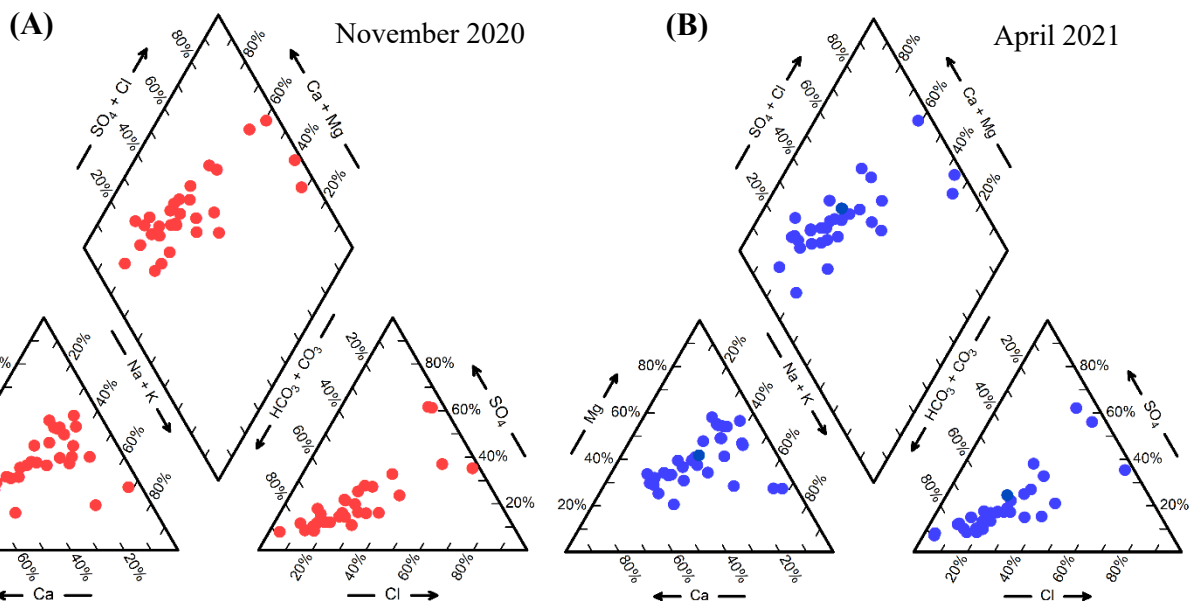
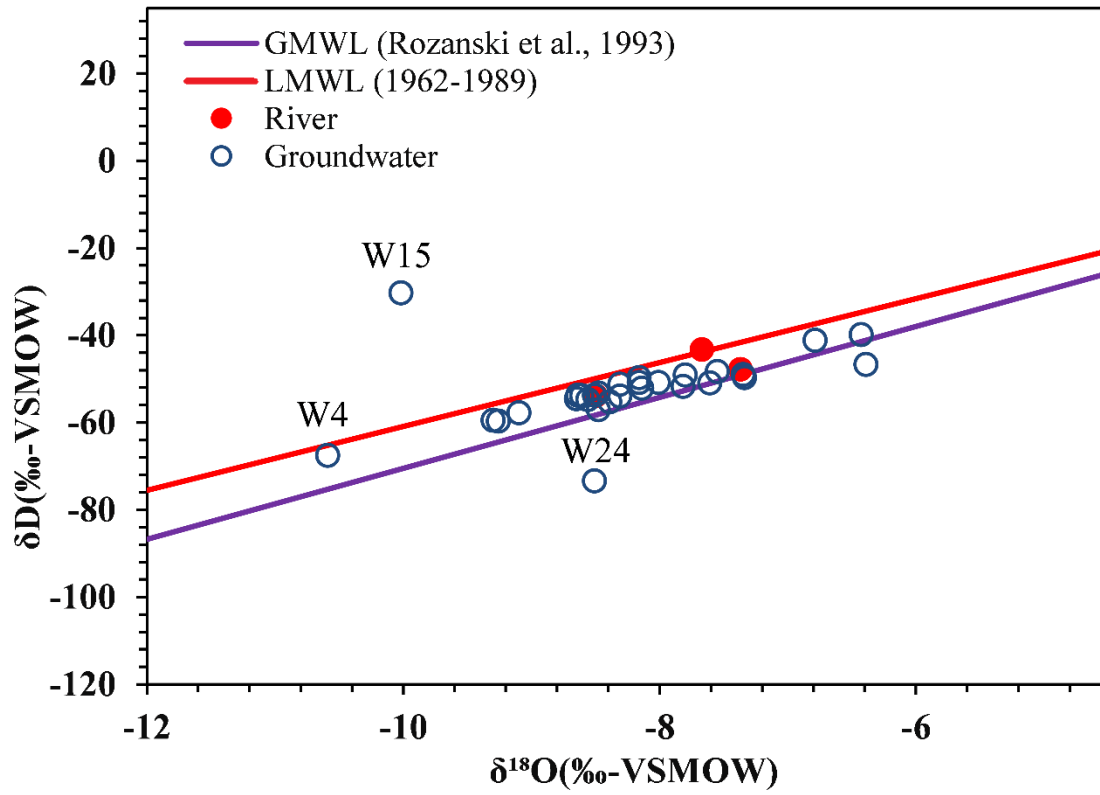


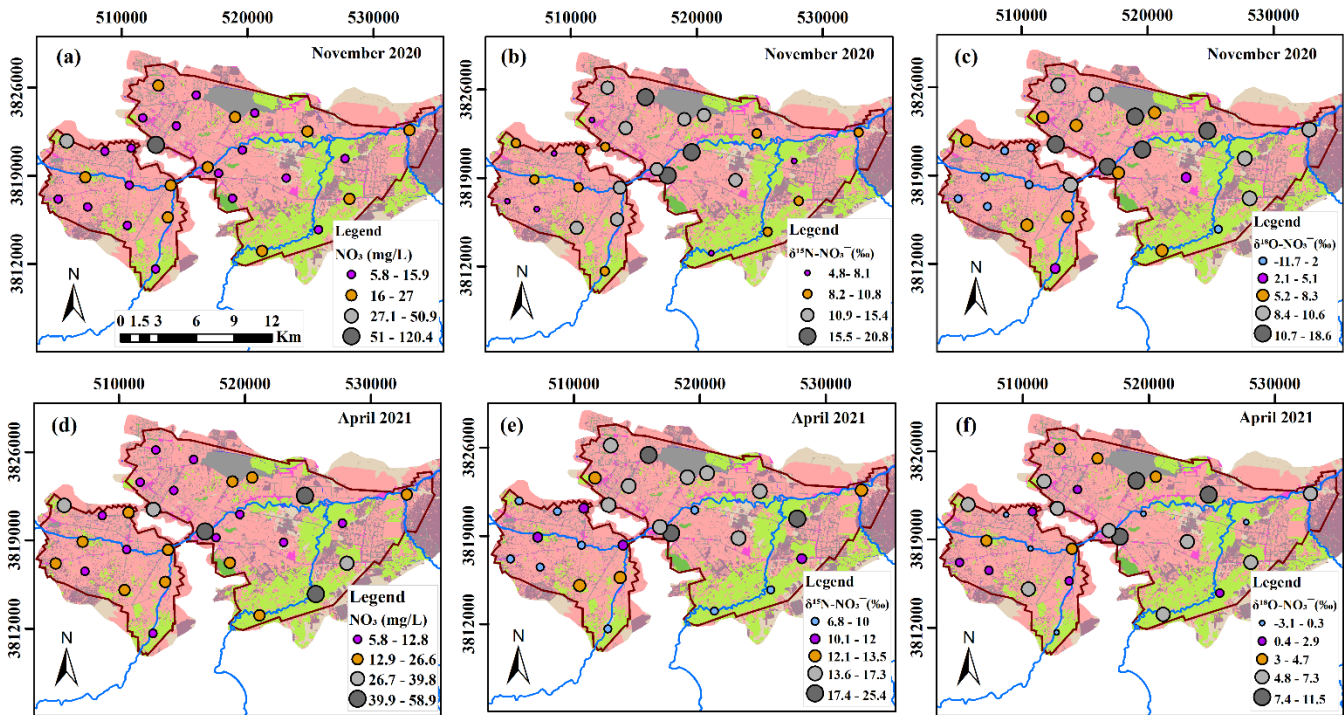
**Fig. 3.** Piper plot showing the chemical compositions of groundwater from the Kabul aquifer in (A) November 2020 and (B) April 2021



860  
861

862 **Fig. 4.**  $\delta^2\text{H-H}_2\text{O}$  vs  $\delta^{18}\text{O-H}_2\text{O}$  plot for the water samples (groundwater and river water) collected from the Kabul  
863 Plain in November 2020 and April 2021.

864  
865



8

**Fig. 5.** Spatial variations of (a and d) nitrate concentrations, (b and e)  $\delta^{15}\text{N-NO}_3^-$  and (c and f)  $\delta^{18}\text{O-NO}_3^-$  values of groundwater samples from the Kabul aquifer collected in the dry season (November 2020) and wet season (April 2021)

869

870

871

872

873

874

875

876

877

878

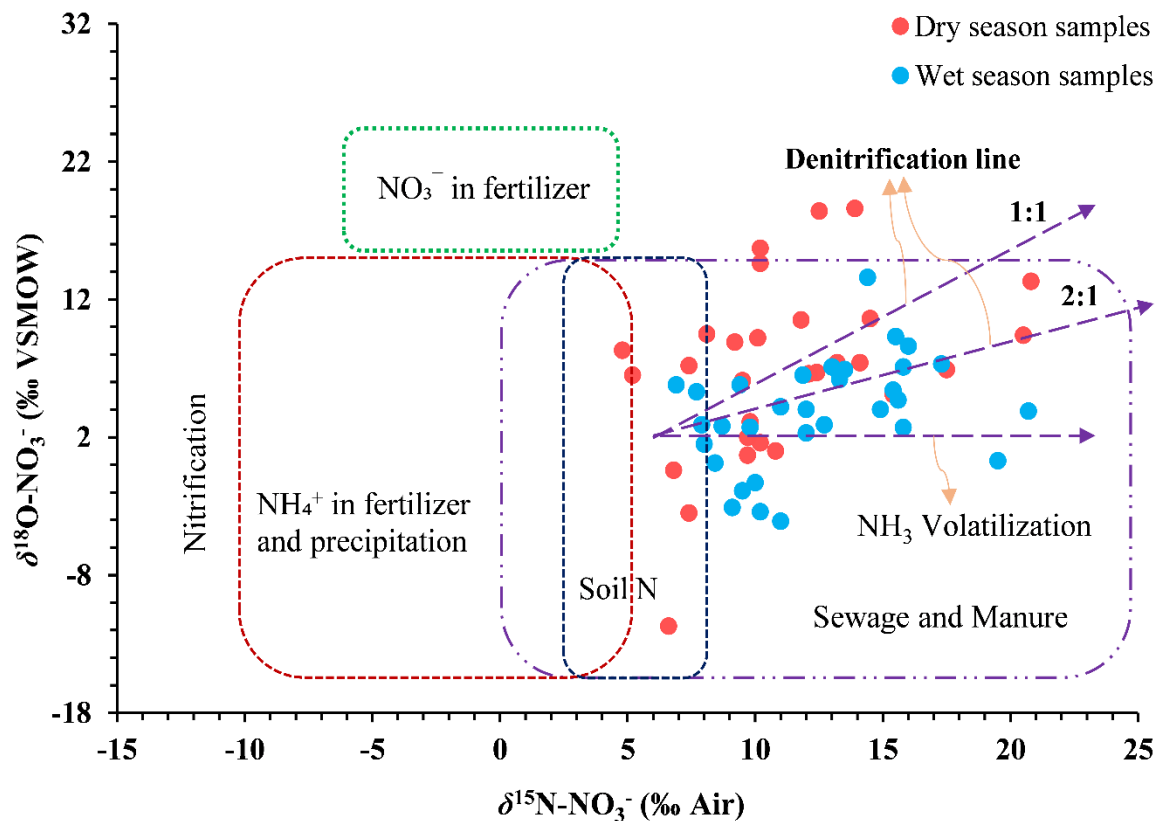
879

880

881

882

883



885

886 **Fig. 6.**  $\delta^{15}\text{N-NO}_3^-$  versus  $\delta^{18}\text{O-NO}_3^-$  in water samples from the Kabul Plain. The typical ranges of isotopic  
 887 compositions are derived from Kendall et al. (2007).

888

889

890

891

892

893

894

895

896

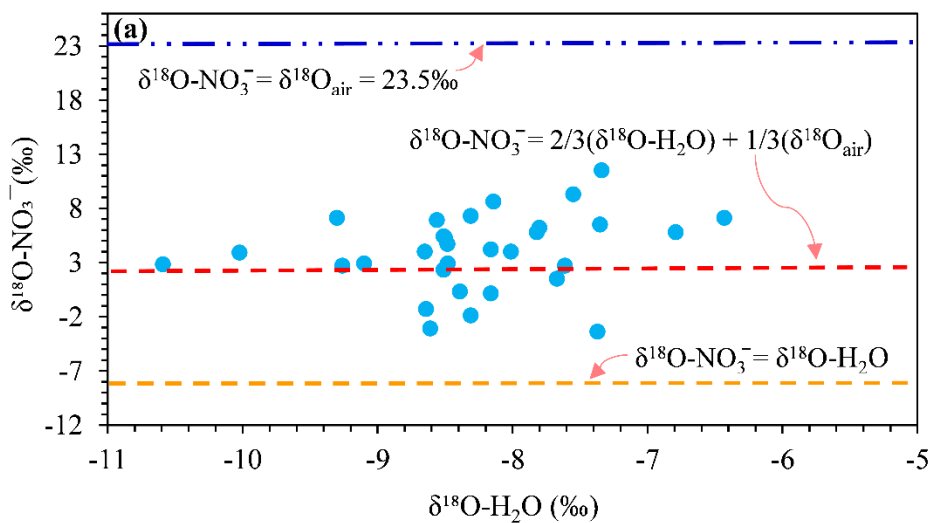
897

898

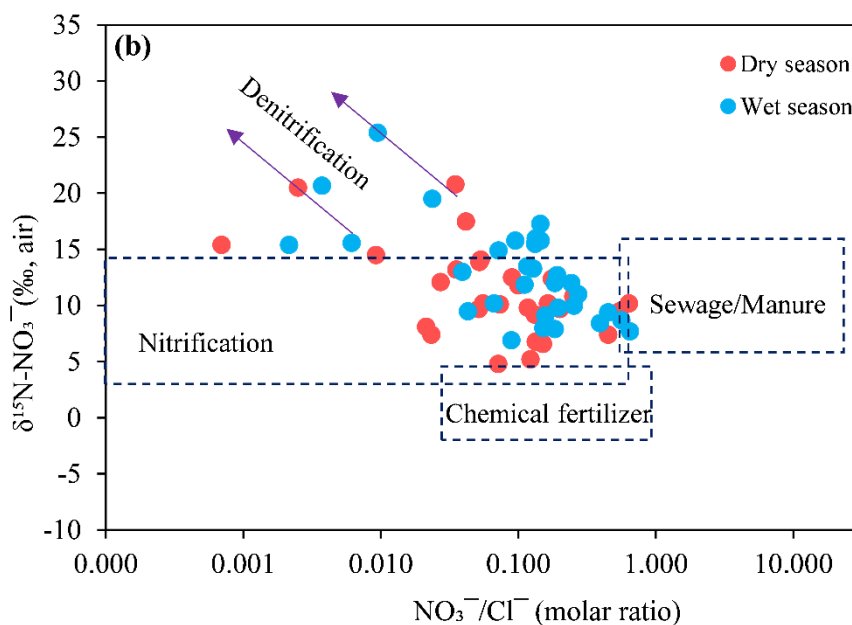
899

900

901  
902



903

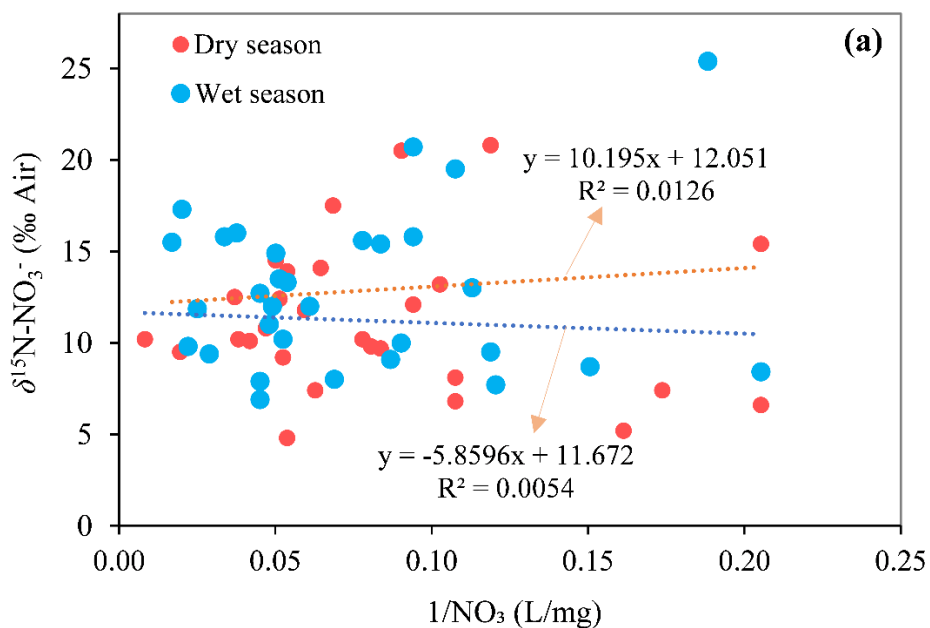


904  
905  
906  
907  
908

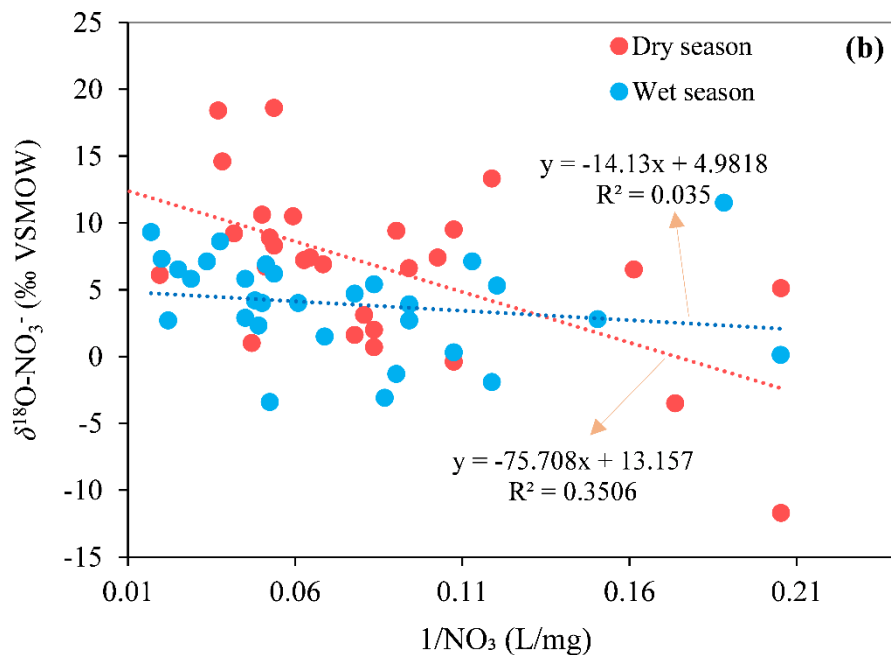
**Fig 7.** Diagrams for identification of nitrification and denitrification processes. (a) Shows  $\delta^{18}\text{O-H}_2\text{O}$  versus  $\delta^{18}\text{O-NO}_3^-$  in water samples from the Kabul Plain, there lines represent the theory line in different conditions and (b) Presents  $\delta^{15}\text{N-NO}_3^-$  versus  $\text{NO}_3^-/\text{Cl}^-$  molar ratio in collected water samples from the Kabul Plain.

909  
910  
911  
912

913  
914

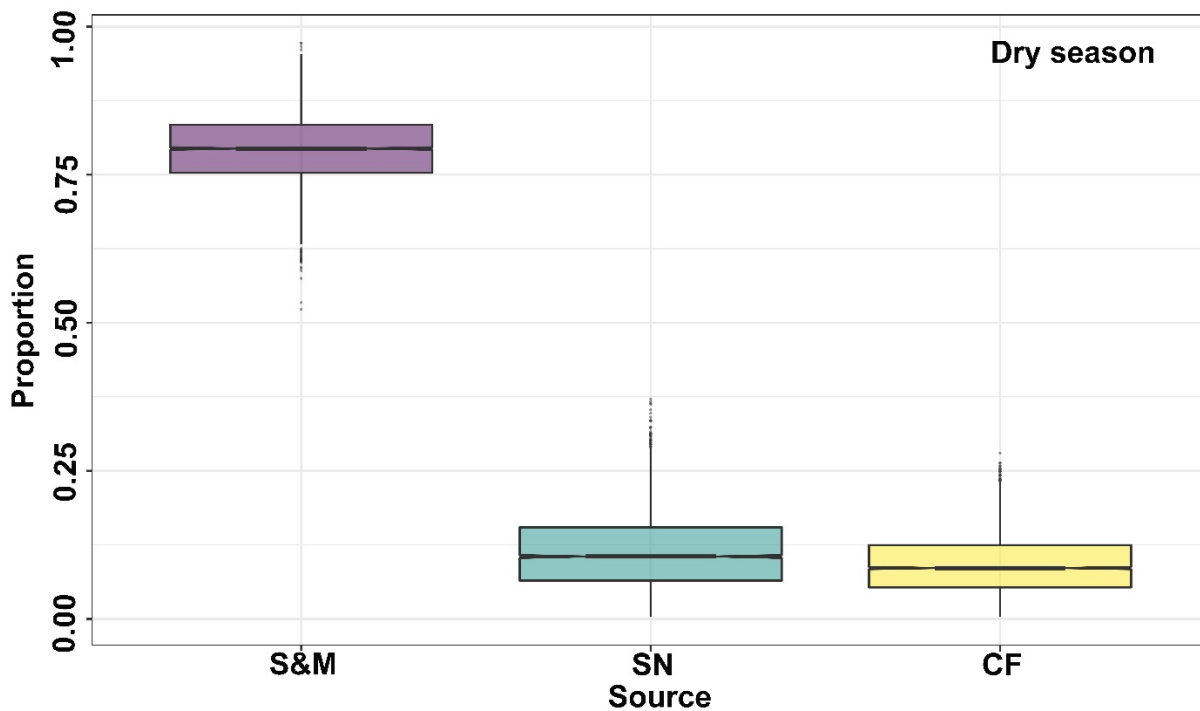


915  
916



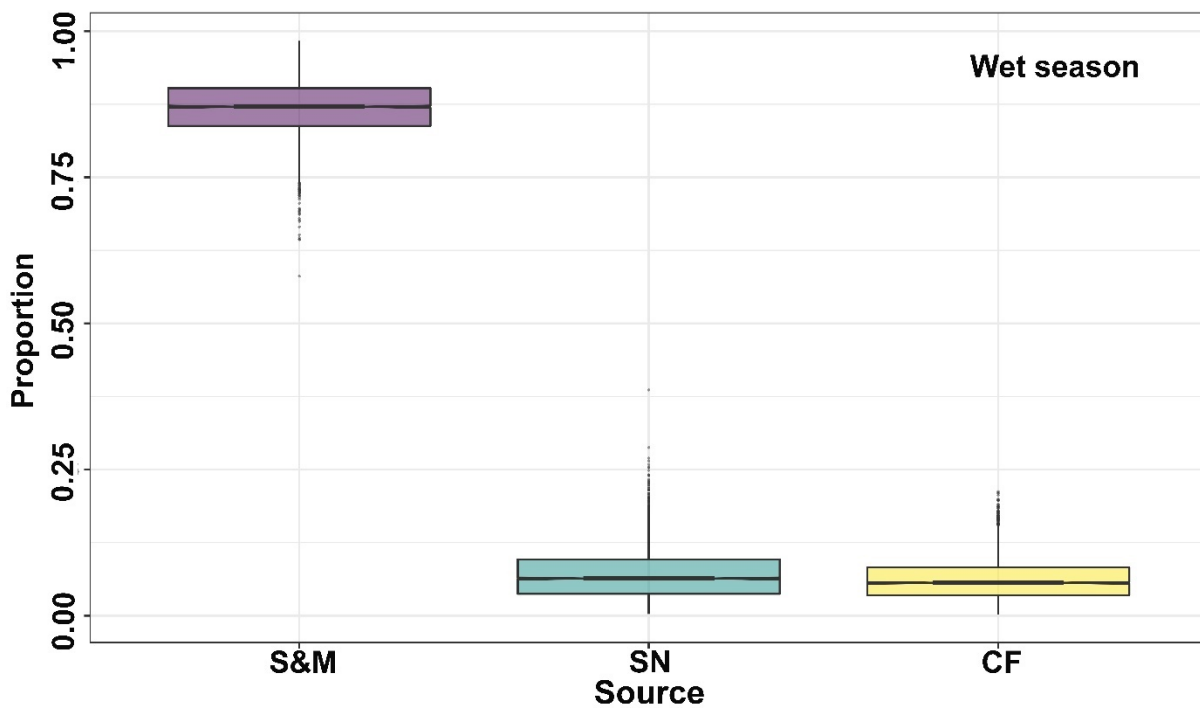
917  
918  
919  
920  
921  
922

**Fig. 8.** Relationship between (a)  $\delta^{15}\text{N-NO}_3^-$  and (b)  $\delta^{18}\text{O-NO}_3^-$  versus  $1/[\text{NO}_3]$  in water samples from the Kabul Plain



923

924



925

926

928 **Fig 9.** Seasonally proportional contributions of three protentional sources of  $\text{NO}_3^-$  in the Kabul aquifer

929 estimated using the SIMMR model (in percentage). Boxplots illustrate the credible interval of 50%

930



932

933

934

935

936 **Highlights**

- 937 • Isotopic analysis was combined with land-use and hydrochemical data to identify the main sources of
- 938 nitrate in the Kabul aquifer.
- 939 • High Cl<sup>-</sup> concentrations and low NO<sub>3</sub><sup>-</sup>/Cl<sup>-</sup> ratios indicated that sewage was the dominant nitrate
- 940 source in the Kabul aquifer.
- 941 • Nitrate processes in the groundwater were mainly derived from nitrification, volatilization.
- 942 • Bayesian stable isotope mixing model: Highest contribution by sewage.

943

944

945

946

947

948

949